ARMY RESEARCH LABORATORY

Linear Theory of a Projectile With a Rotating Internal Part in Atmospheric Flight

by Geoffrey Frost and Mark Costello

ARL-CR-530 **July 2003**

prepared by

Geoffrey Frost and Mark Costello
Oregon State University
Corvallis, OR 97331

under contract

DAAD17-02-P-1104

NOTICES

Disclaimers

The findings in this report are not to be construed as an official Department of the Army position unless so designated by other authorized documents.

Citation of manufacturer's or trade names does not constitute an official endorsement or approval of the use thereof.

Destroy this report when it is no longer needed. Do not return it to the originator.

Army Research Laboratory
Aberdeen Proving Ground, MD 21005-5066

ARL-CR-530 **July 2003**

Linear Theory of a Projectile With a Rotating Internal Part in Atmospheric Flight

Geoffrey Frost and Mark Costello
Oregon State University

prepared by

Geoffrey Frost and Mark Costello
Oregon State University
Corvallis, OR 97331

under contract

DAAD17-02-P-1104

Report Documentation Page

Form Approved
OMB No. 0704-0188

1. REPORT DATE *(DD-MM-YYYY)*	2. REPORT TYPE	3. DATES COVERED (From - To)
July 2003	Final	May 2002–May 2003

4. TITLE AND SUBTITLE
Linear Theory of a Projectile With a Rotating Internal Part in Atmospheric Flight

5a. CONTRACT NUMBER
DAAD17-02-P-1104

5b. GRANT NUMBER

5c. PROGRAM ELEMENT NUMBER

6. AUTHOR(S)
Geoffrey Frost and Mark Costello

5d. PROJECT NUMBER

5e. TASK NUMBER

5f. WORK UNIT NUMBER

7. PERFORMING ORGANIZATION NAME(S) AND ADDRESS(ES)
Oregon State University
Department of Mechanical Engineering
Corvallis, OR 97331

8. PERFORMING ORGANIZATION REPORT NUMBER

9. SPONSORING/MONITORING AGENCY NAME(S) AND ADDRESS(ES)
U.S. Army Research Laboratory
ATTN: AMSRL-WM-BC
Aberdeen Proving Ground, MD 21005-5066

10. SPONSOR/MONITOR'S ACRONYM(S)

11. SPONSOR/MONITOR'S REPORT NUMBER(S)
ARL-CR-530

12. DISTRIBUTION/AVAILABILITY STATEMENT
Approved for public release; distribution is unlimited.

13. SUPPLEMENTARY NOTES

14. ABSTRACT
Dynamic modeling of the atmospheric flight mechanics of a projectile equipped with an internal rotating disk is investigated and a modified projectile linear theory is established for this configuration. To model this type of projectile requires alteration of several of the coefficients of the epicyclic dynamics leading to changes in the fast and slow epicyclic modes. A study of the frequency and damping properties of the epicyclic modes is conducted by systematically varying disk mass, rotational speed, and location. It is shown that the presence of an internal rotating disk can cause substantial changes in the epicyclic dynamics, including instability, in some configurations.

15. SUBJECT TERMS
flight dynamics, projectile linear theory

16. SECURITY CLASSIFICATION OF:			17. LIMITATION OF ABSTRACT	18. NUMBER OF PAGES	19a. NAME OF RESPONSIBLE PERSON
a. REPORT	b. ABSTRACT	c. THIS PAGE			Peter Plostins
UNCLASSIFIED	UNCLASSIFIED	UNCLASSIFIED	UL	52	19b. TELEPHONE NUMBER (*Include area code*) 410-278-8878

Standard Form 298 (Rev. 8/98)
Prescribed by ANSI Std. Z39.18

Contents

List of Figures

1. Introduction

Many conventional projectile configurations contain internal parts that slightly move in flight in some way, shape, or form. Fuze mechanisms used on some indirect fire ammunition employ a rotor that is permitted to move slightly with respect to the main projectile body. Submunitions deployed from indirect fire projectiles are keyed into place inside the round; however, small relative motion between parts occurs. These configurations can experience dynamic instability typified by large loss in range and large spin decay (*1*). Soper (*2*) evaluated the stability of a spinning projectile that contains a cylindrical mass fitted loosely into a cylindrical cavity. The cylinder is constrained to spin with the main body projectile. It is shown that an unstable coning motion exists in which spin decay and cone angle grow proportional to friction coefficient between the mass and cavity and the maximum cant angle between the mass and the projectile. Using a similar geometric configuration, Murphy (*3*) developed a quasi-linear solution for a projectile with an internal moving part. It provided an explanation of the unusual flight behavior exhibited by four projectiles that all contained parts with slight relative motion between components. Later, D'Amico (*4*) performed a detailed series of experiments where a projectile with a loose internal part was driven by the rotor of a freely gimbaled gyroscope. The gyroscope yaw history and the orbital motion of the loose part were measured and used to predict the moment and resulting yaw growth caused by the loose part. Hodapp (*5*) expanded the work of Soper and Murphy (*2, 3*) by considering a projectile configuration with a partially restrained internal member with a mass center offset. Results of this study indicate that small mass center offset of the partially restrained internal member can reduce the instability caused by the loose internal part.

New projectiles configurations have emerged that contain multiple moving parts which are fundamental to the basic design and operation of the projectile. The gimbal nose projectile configuration is an example of one such configuration. It consists of a standard projectile shape with a nose section that is free to rotate with respect to the main body. Goddard (*6*) originally conceived this device for aircraft control, and later Barrett and Stutts (*7*) considered this mechanism for active control of munitions. Schmidt and Donovan (*8*) as well as Costello and Agarwalla (*9*) showed that dispersion of a fin-stabilized direct fire projectile could be reduced by more than 50% using a passive gimbal nose to significantly reduce aerodynamic jump. Another multiple component configuration is the dual-spin projectile, which consists of forward and aft sections connected through a bearing, allowing different spin rates for each section. Smith et al. (*10*) used a dual-spin projectile for active control of an artillery shell by mounting canards on the forward section of the projectile. The forward section was roll stabilized to aid the functionality of the canards while the aft section provided spin stability. Costello and Peterson (*11*) developed a linear theory for dual-spin projectiles that predicts stability for this configuration while Burchett et al. (*12*) predicted swerve of a dual-spin projectile caused by lateral pulse jets.

An internal rotating disk is an important dynamic component of some new projectile configurations. For example, a new concept for generating real-time bomb damage information relies on releasing a relatively small sensor projectile that is tethered to a parent bomb. As the two projectiles separate, a reel on the parent munition spins. In another application, active trajectory control is achieved by controlling the spin rate of the external projectile body, thus predictably changing the aerodynamic loads. To implement this control concept requires an internal rotating disk. In these cases, weapon system designers require guidance on the effect of the rotating internal part as well as guidance on how to optimally configure such a system. The work reported here sheds light on these matters by first developing a projectile linear theory specific to projectiles with an internal rotating disk. This is followed by a study of the effect of the physical parameters such as the placement, orientation, mass, and speed of the rotating disk on the epicyclic modes of vibration.

2. Rotating Internal Part Projectile Dynamic Model

A projectile containing an axisymmetric rotating internal part that spins at a constant rate, Ω, is considered as shown in Figure 1. The mathematical model describing the motion of the projectile allows for three translational and three rotational rigid-body degrees of freedom. In order to develop the dynamic equations of motion for these six degrees of freedom, three separate reference frames are used as shown in Figure 1. The ground surface is used as an inertial reference frame with $\vec{K}_I$ positive down. A body frame is fixed on the projectile at the mass center of the two-body system with $\vec{I}_B$ positive out the nose of the projectile. Due to the axisymmetric nature of the rotating internal part, the mass center of the internal part is fixed with respect to the body frame. The disk is considered to have a known constant spin rate, and its axis of spin is specified in the body frame by a set of direction cosine elements.

The three translational degrees of freedom are the three components of the two-body, mass center position vector.

$$\vec{r}_{O\to C} = x\vec{I}_I + y\vec{J}_I + z\vec{K}_I . \tag{1}$$

A sequence of rotations from the inertial frame to the projectile frame is defined by a set of body-fixed rotations that are ordered in the conventional manner as shown in Figure 2. The three rotational degrees of freedom are the Euler roll angle (ϕ), pitch angle (θ), and yaw angle (ψ). In the normal process of simplifying the equations of motion using projectile linear theory, an intermediate frame is utilized, namely, the no-roll frame, defined as an intermediate frame before roll angle rotation. Figure 3 shows the relative locations of the projectile and disk centers of gravity and the projectile body centers of pressure.

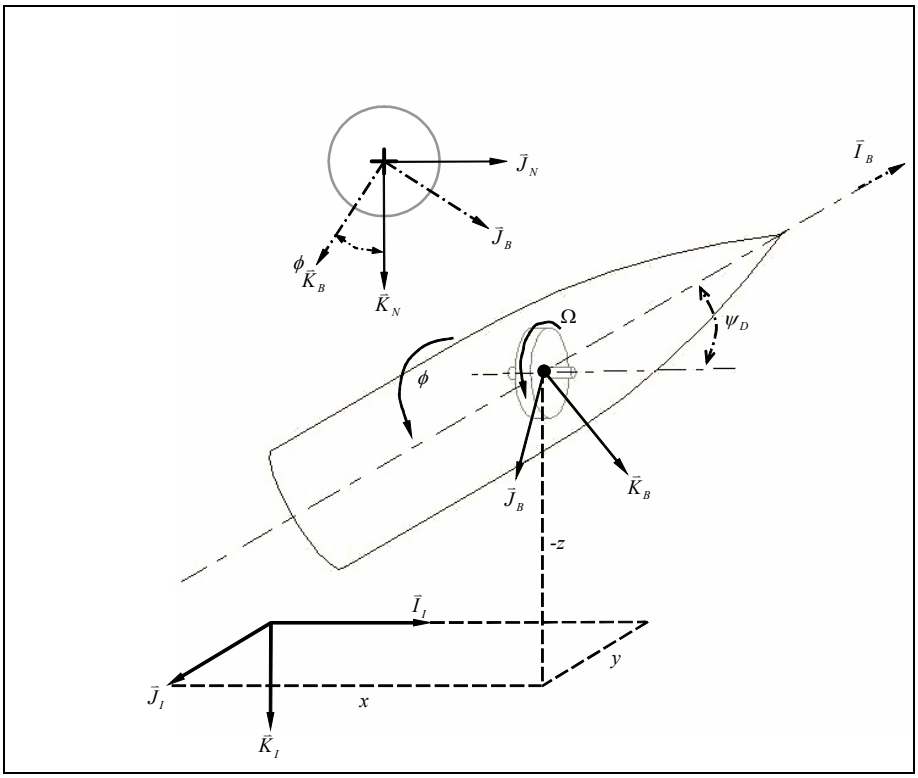

Figure 1. Position coordinates schematic of a rotating internal part projectile.

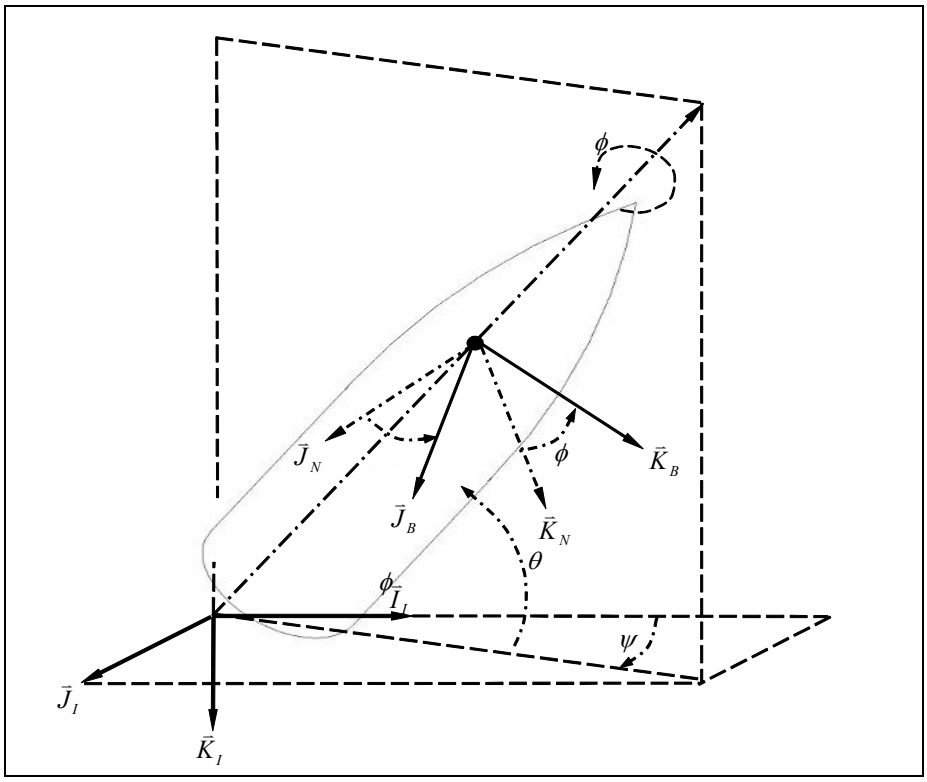

Figure 2. Attitude coordinates schematic of a rotating internal part projectile.

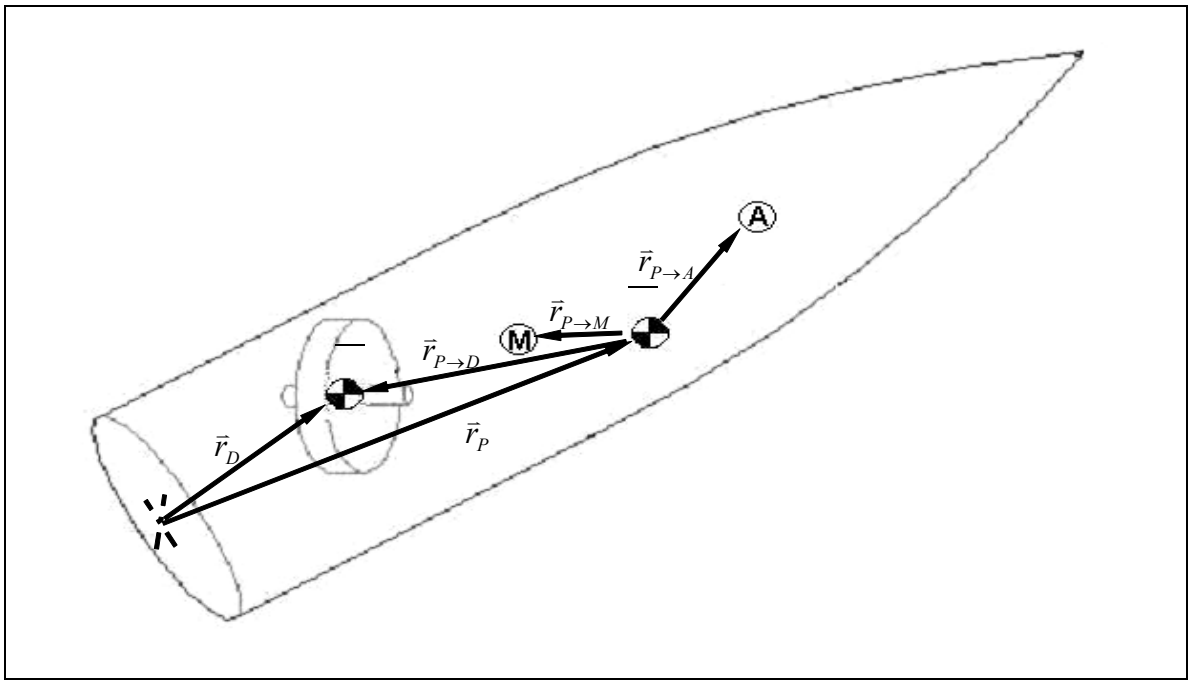

Figure 3. Rotating internal part projectile geometry.

The kinematic differential equations define 6 of the 12 dynamic equations needed to describe the motion of the states: x, y, z, φ, θ, and ψ. The no-roll variables, $\widetilde{u},\widetilde{v},\widetilde{w},\widetilde{p},\widetilde{q},$ and $\widetilde{r}$, are chosen for the remaining 12 state variables. The transformation from the no-roll frame (N) to the inertial frame (I) is

$$\begin{Bmatrix}\vec{I}_I\\ \vec{J}_I\\ \vec{K}_I\end{Bmatrix}=\begin{bmatrix}c_\theta c_\psi & -s_\psi & s_\theta c_\psi\\ c_\theta s_\psi & c_\psi & s_\theta s_\psi\\ -s_\theta & 0 & c_\theta\end{bmatrix}\begin{Bmatrix}\vec{I}_N\\ \vec{J}_N\\ \vec{K}_N\end{Bmatrix}=\left[T_N\right]\begin{Bmatrix}\vec{I}_N\\ \vec{J}_N\\ \vec{K}_N\end{Bmatrix}, \tag{2}$$

while the transformation from the projectile body frame, (B), to the no-roll frame, (N), is

$$\begin{Bmatrix}\vec{I}_N\\ \vec{J}_N\\ \vec{K}_N\end{Bmatrix}=\begin{bmatrix}1 & 0 & 0\\ 0 & c_\phi & -s_\phi\\ 0 & s_\phi & c_\phi\end{bmatrix}\begin{Bmatrix}\vec{I}_B\\ \vec{J}_B\\ \vec{K}_B\end{Bmatrix}=\left[T_\phi\right]\begin{Bmatrix}\vec{I}_B\\ \vec{J}_B\\ \vec{K}_B\end{Bmatrix}, \tag{3}$$

leading to the transformation from the body frame (B) to the inertial frame (I) described by

$$\begin{Bmatrix}\vec{I}_I\\ \vec{J}_I\\ \vec{K}_I\end{Bmatrix}=\begin{bmatrix}c_\theta c_\psi & s_\phi s_\theta c_\psi - c_\phi s_\psi & c_\phi s_\theta c_\psi + s_\phi s_\psi\\ c_\theta s_\psi & s_\phi s_\theta s_\psi + c_\phi c_\psi & c_\phi s_\theta s_\psi - s_\phi c_\psi\\ -s_\theta & s_\phi c_\theta & c_\phi c_\theta\end{bmatrix}\begin{Bmatrix}\vec{I}_B\\ \vec{J}_B\\ \vec{K}_B\end{Bmatrix}=\left[T_B\right]\begin{Bmatrix}\vec{I}_B\\ \vec{J}_B\\ \vec{K}_B\end{Bmatrix}. \tag{4}$$

In the above equations and the equations shown below, the standard shorthand notation for trigonometric functions is used: $\sin(\alpha)\equiv s_\alpha$, $\cos(\alpha)\equiv c_\alpha$, $\tan(\alpha)\equiv t_\alpha$.

The mass center velocity vector of the two-body system is defined in each of the reference frames previously discussed,

$$\vec{v}_{C/I} = \tilde{u}\vec{I}_N + \tilde{v}\vec{J}_N + \tilde{w}\vec{K}_N = u\vec{I}_B + v\vec{J}_B + w\vec{K}_B = \dot{x}\vec{I}_I + \dot{y}\vec{J}_I + \dot{z}\vec{K}_I\,, \tag{5}$$

as is the angular velocity vector of the projectile body,

$$\vec{\omega}_{B/I} = \tilde{p}\vec{I}_N + \tilde{q}\vec{J}_N + \tilde{r}\vec{K}_N = p\vec{I}_B + q\vec{J}_B + r\vec{K}_B\,, \tag{6}$$

and the angular velocity vector of the no-roll reference frame,

$$\vec{\omega}_{N/I} = -\tilde{r}t_\theta\vec{I}_N + \tilde{q}\vec{J}_N + \tilde{r}\vec{K}_{NB}\,. \tag{7}$$

The angular velocity vector of the internal rotating part with respect to the inertial frame is found by summing the angular velocity vector of the projectile body with respect to the inertial frame with the angular velocity vector of the internal rotating part with respect to the projectile body frame:

$$\vec{\omega}_{D/I} = \vec{\omega}_{B/I} + \vec{\omega}_{D/B}\,, \tag{8}$$

where the angular velocity vector of the internal rotating part with respect to the projectile body frame is

$$\vec{\omega}_{D/P} = n_x\Omega\vec{I}_B + n_y\Omega\vec{J}_B + n_z\Omega\vec{K}_B\,. \tag{9}$$

Applying the transformation given in equation 2 to the mass center velocity components expressed in the no-roll reference frame yields

$$\begin{Bmatrix}\dot{x}\\ \dot{y}\\ \dot{z}\end{Bmatrix} = \begin{bmatrix} c_\theta c_\psi & -s_\psi & s_\theta c_\psi \\ c_\theta s_\psi & c_\psi & s_\theta s_\psi \\ -s_\theta & 0 & c_\theta \end{bmatrix}\begin{Bmatrix}\tilde{u}\\ \tilde{v}\\ \tilde{w}\end{Bmatrix}. \tag{10}$$

Equating the projectile angular velocity vectors described using no-roll frame components and using Euler angle rates generates

$$\begin{Bmatrix}\dot{\phi}\\ \dot{\theta}\\ \dot{\psi}\end{Bmatrix} = \begin{bmatrix} 1 & 0 & t_\theta \\ 0 & 1 & 0 \\ 0 & 0 & 1/c_\theta \end{bmatrix}\begin{Bmatrix}\tilde{p}\\ \tilde{q}\\ \tilde{r}\end{Bmatrix}. \tag{11}$$

The kinetic differential equations are derived by separating the two-body system at the disk axle connection points and considering the reaction forces and moments associated with each individual part. A constraint force $\vec{F}_R$ and a constraint moment $\vec{M}_R$, applied at the disk center of gravity, couple the disk and projectile bodies. The translational kinetic differential equations for each body are given by equations 12 and 13:

$$m_D \vec{a}_{D/I} = \vec{F}_R + \vec{W}_D ; \tag{12}$$

$$m_P \vec{a}_{P/I} = -\vec{F}_R + \vec{W}_P + \vec{F}_A . \tag{13}$$

Summing equations 12 and 13 yields the expression for the translational dynamic equation of motion for the two-body system,

$$m_C \vec{a}_{C/I} = \vec{F}_A + \vec{W}_C , \tag{14}$$

where

$$m_C \vec{a}_{C/I} = m_D \vec{a}_{D/I} + m_P \vec{a}_{P/I} \tag{15}$$

and

$$\vec{W}_C = \vec{W}_P + \vec{W}_D ; \tag{16}$$

$$\vec{a}_{C/I} = \frac{{}^N d\vec{V}_{C/I}}{dt} + \vec{\omega}_{N/I} \times \vec{V}_{C/I} . \tag{17}$$

The constraint force is obtained by subtracting equation 13 from equation 12:

$$\vec{F}_R = \left(\vec{a}_{D/I} - \vec{a}_{P/I} + \frac{\vec{F}_A}{m_P} \right) \left(\frac{m_D m_P}{m_D + m_P} \right). \tag{18}$$

The acceleration of the mass center of the disk, $\vec{a}_{D/I}$, can be expressed in terms of the acceleration of the projectile mass center by using the formula for two points fixed on a rigid body.

$$\vec{a}_{D/I} = \vec{a}_{P/I} + \vec{\alpha}_{P/I} \times \vec{r}_{P \to D} + \vec{\omega}_{P/I} \times (\vec{\omega}_{P/I} \times \vec{r}_{P \to D}) . \tag{19}$$

After substituting this expression into equation 18, the constraint force is expressed in the following manner:

$$\vec{F}_R = \left(\vec{\alpha}_{P/I} \times \vec{r}_{P \to D} + \vec{\omega}_{P/I} \times (\vec{\omega}_{P/I} \times \vec{r}_{P \to D}) + \frac{\vec{F}_A}{m_P} \right) \left(\frac{m_D m_P}{m_D + m_P} \right). \tag{20}$$

The rotational kinetic equations of motion for the projectile and disk bodies are given by

$$\frac{{}^I d\vec{H}_{D/I}}{dt} = \vec{M}_R ; \tag{21}$$

$$\frac{{}^I d\vec{H}_{P/I}}{dt} = -\vec{M}_R - \vec{r}_{P \to D} \times \vec{F}_R + \vec{M}_A . \tag{22}$$

Summing equations 21 and 22 eliminates the reaction moment and forms the rotational kinetic equation for the two-body system expressed in the body reference frame.

$$\frac{{}^{I}d\vec{H}_{P/I}}{dt} + \frac{{}^{I}d\vec{H}_{D/I}}{dt} = -\vec{r}_{P\to D} \times \vec{F}_R + \vec{M}_A \,. \tag{23}$$

Unlike the kinetic translational equation of motion, it is easier to form the rotational equation of motion in the body frame and later convert it to the no-roll reference frame when expressing in component form. Therefore, the angular momentum derivatives are expressed as

$$\frac{{}^{I}d\vec{H}_{D/I}}{dt} = \frac{{}^{B}d\vec{H}_{D/I}}{dt} + \omega_{B/I} \times \vec{H}_{D/I}\,; \tag{24}$$

$$\frac{{}^{I}d\vec{H}_{P/I}}{dt} = \frac{{}^{B}d\vec{H}_{P/I}}{dt} + \omega_{B/I} \times \vec{H}_{P/I}\,. \tag{25}$$

The translational dynamic equation given in equation 26 is expressed in the no-roll frame.

$$\begin{Bmatrix} \dot{\widetilde{u}} \\ \dot{\widetilde{v}} \\ \dot{\widetilde{w}} \end{Bmatrix} = \frac{1}{m_C} \begin{Bmatrix} \widetilde{X} \\ \widetilde{Y} \\ \widetilde{Z} \end{Bmatrix} - \begin{bmatrix} 0 & -\widetilde{r} & \widetilde{q} \\ \widetilde{r} & 0 & \widetilde{r}t_\theta \\ -\widetilde{q} & -\widetilde{r}t_\theta & 0 \end{bmatrix} \begin{Bmatrix} \widetilde{u} \\ \widetilde{v} \\ \widetilde{w} \end{Bmatrix}, \tag{26}$$

where the weight force and aerodynamic loads expressed in the no-roll frame are written as

$$\vec{F}_A = \widetilde{X}_A \vec{I}_N + \widetilde{Y}_A \vec{J}_N + \widetilde{Z}_A \vec{K}_N\,; \tag{27}$$

$$\vec{W}_C = \widetilde{X}_W \vec{I}_N + \widetilde{Y}_W \vec{J}_N + \widetilde{Z}_W \vec{K}_N\,, \tag{28}$$

so that

$$\begin{Bmatrix} \widetilde{X} \\ \widetilde{Y} \\ \widetilde{Z} \end{Bmatrix} = \begin{Bmatrix} \widetilde{X}_A \\ \widetilde{Y}_A \\ \widetilde{Z}_A \end{Bmatrix} + \begin{Bmatrix} \widetilde{X}_W \\ \widetilde{Y}_W \\ \widetilde{Z}_W \end{Bmatrix}, \tag{29}$$

where

$$\begin{Bmatrix} \widetilde{X}_W \\ \widetilde{Y}_W \\ \widetilde{Z}_W \end{Bmatrix} = m_C g \begin{Bmatrix} -s_\theta \\ 0 \\ c_\theta \end{Bmatrix}. \tag{30}$$

The aerodynamic forces are described in section 3.

The body frame components of the rotational dynamics equation of motion given by equation 23 can be written as

$$\left[A_{RD}\right]\begin{Bmatrix}\dot{p}\\ \dot{q}\\ \dot{r}\end{Bmatrix}=\left\{B_{RD}\right\}, \tag{31}$$

where

$$A_{RD}=I_P+T_D^T I_D T_D-m_S S_{RPD}S_{RPD}; \tag{32}$$

$$B_{RD}=\begin{Bmatrix}L_A\\ M_A\\ N_A\end{Bmatrix}-m_s S_{RPD}S_\omega S_\omega\begin{Bmatrix}x_{PD}\\ y_{PD}\\ z_{PD}\end{Bmatrix}-\frac{m_S}{m_P}S_{RPD}\begin{Bmatrix}X_A\\ Y_A\\ Z_A\end{Bmatrix}-S_\omega I_P\begin{Bmatrix}p\\ q\\ r\end{Bmatrix}-S_\omega T_D^T I_D T_D\begin{Bmatrix}p+n_x\Omega\\ q+n_y\Omega\\ r+n_z\Omega\end{Bmatrix}; \tag{33}$$

and

$$S_{RPD}=\begin{bmatrix}0 & -z_{PD} & y_{PD}\\ z_{PD} & 0 & -x_{PD}\\ -y_{PD} & x_{PD} & 0\end{bmatrix}; \tag{34}$$

$$\left[S_\omega\right]=\begin{bmatrix}0 & -r & q\\ r & 0 & -p\\ -q & p & 0\end{bmatrix}. \tag{35}$$

The unit vectors, n_x, n_y, and n_z, are the set of direction cosine elements that specify the axis of spin of the disk in the body frame.

To be consistent with projectile linear theory, equation 31 is converted to the no-roll frame through multiplication of the equation by T_ϕ^T. Also, a change of variables is introduced from body frame angular velocity components to no-roll frame components. With these conversions, equation 31 is expressed as

$$\left[\widetilde{A}_{RD}\right]\begin{Bmatrix}\dot{\tilde{p}}\\ \dot{\tilde{q}}\\ \dot{\tilde{r}}\end{Bmatrix}=\left\{\widetilde{B}_{RD}\right\}, \tag{36}$$

where

$$\widetilde{A}_{RD}=T_\phi^T\left(I_P+T_D^T I_D T_D-m_S S_{RPD}S_{RPD}\right)T_\phi\ , \tag{37}$$

$$\widetilde{B}_{RD} = \begin{Bmatrix} \widetilde{L}_A \\ \widetilde{M}_A \\ \widetilde{N}_A \end{Bmatrix} - m_S T_\phi^T S_{RPD} S_\omega S_\omega \begin{Bmatrix} x_{PD} \\ y_{PD} \\ z_{PD} \end{Bmatrix} - \frac{m_S}{m_P} T_\phi^T S_{RPD} \begin{Bmatrix} \widetilde{X}_A \\ \widetilde{Y}_A \\ \widetilde{Z}_A \end{Bmatrix} - T_\phi^T S_\omega I_P T_\phi \begin{Bmatrix} \widetilde{p} \\ \widetilde{q} \\ \widetilde{r} \end{Bmatrix}$$

$$- T_\phi^T S_\omega T_D^T I_D T_D T_\phi \begin{Bmatrix} \widetilde{p} \\ \widetilde{q} \\ \widetilde{r} \end{Bmatrix} - T_\phi^T S_\omega T_D^T I_D T_D \begin{Bmatrix} n_x \Omega \\ n_y \Omega \\ n_z \Omega \end{Bmatrix} - T_\phi^T \left(I_P + T_D^T I_D T_D - m_S S_{RPD} S_{RPD} \right) \dot{T}_\phi \begin{Bmatrix} \widetilde{p} \\ \widetilde{q} \\ \widetilde{r} \end{Bmatrix}, \quad (38)$$

and

$$T_\phi = \begin{bmatrix} 1 & 0 & 0 \\ 0 & c_\phi & s_\phi \\ 0 & -s_\phi & c_\phi \end{bmatrix}; \quad (39)$$

$$\dot{T}_\phi = \left(\widetilde{p} + t_\theta \widetilde{r} \right) \begin{bmatrix} 0 & 0 & 0 \\ 0 & -s_\phi & c_\phi \\ 0 & -c_\phi & -s_\phi \end{bmatrix}. \quad (40)$$

In the cross product operator matrix, S_ω, in equation 38, the body frame angular velocity components *p*, *q*, and *r* are replaced by $\widetilde{p}$, $c_\phi \widetilde{q} + s_\phi \widetilde{r}$, and $-s_\phi \widetilde{q} + c_\phi \widetilde{r}$, respectively.

Equations 10, 11, 26, and 36 provide 12 nonlinear differential equations that govern atmospheric flight of a projectile equipped with an axisymmetric rotating internal component. With a given set of initial conditions, these equations can be numerically integrated forward in time.

3. Aerodynamic Forces and Moments

The equations of motion previously discussed are largely driven by the aerodynamic forces and moments exerted on the projectile body. The aerodynamic loads consist of steady aerodynamic forces and linear Magnus forces and are formulated separately.

$$\begin{Bmatrix} \widetilde{X}_A \\ \widetilde{Y}_A \\ \widetilde{Z}_A \end{Bmatrix} = \begin{Bmatrix} \widetilde{X}_S \\ \widetilde{Y}_S \\ \widetilde{Z}_S \end{Bmatrix} + \begin{Bmatrix} \widetilde{X}_M \\ \widetilde{Y}_M \\ \widetilde{Z}_M \end{Bmatrix}. \quad (41)$$

The steady aerodynamic forces act at the center of pressure of the projectile body and are provided in equation 42:

$$\begin{Bmatrix} \widetilde{X}_S \\ \widetilde{Y}_S \\ \widetilde{Z}_S \end{Bmatrix} = -q_\alpha \begin{Bmatrix} C_{X0} + C_{X2}\alpha^2 + C_{X2}\beta^2 \\ C_{Y0} + C_{YB1}\beta \\ C_{Z0} + C_{ZB1}\alpha \end{Bmatrix}. \tag{42}$$

The Magnus force acts at the Magnus force center of pressure, which is different from the center of pressure of the steady aerodynamic forces. Figure 3 shows the relative locations of the projectile body centers of pressure.

$$\begin{Bmatrix} \widetilde{X}_M \\ \widetilde{Y}_M \\ \widetilde{Z}_M \end{Bmatrix} = q_\alpha \begin{Bmatrix} 0 \\ \dfrac{\widetilde{p}DC_{YPA}\alpha}{2V} \\ -\dfrac{\widetilde{p}DC_{YPA}\beta}{2V} \end{Bmatrix}. \tag{43}$$

The longitudinal and lateral aerodynamic angles of attack used in equations 42 and 43 are given in equation 44:

$$\alpha = \tan^{-1}(\widetilde{w}/\widetilde{u}) \cong \widetilde{w}/\widetilde{u} \qquad \beta = \tan^{-1}(\widetilde{v}/\widetilde{u}) \cong \widetilde{v}/\widetilde{u}\,; \tag{44}$$

$$q_\alpha = \frac{\pi}{8}\rho D^2(\widetilde{u}^2 + \widetilde{v}^2 + \widetilde{w}^2)\,. \tag{45}$$

Aerodynamic coefficients in equations 42 and 43 depend on the local Mach number at the projectile mass center.

The externally applied moments on the projectile body found on the right-hand side of the rotational kinetic equations contain contributions from steady and unsteady aerodynamics and Magnus moments.

$$\begin{Bmatrix} \widetilde{L}_A \\ \widetilde{M}_A \\ \widetilde{N}_A \end{Bmatrix} = \begin{Bmatrix} \widetilde{L}_S \\ \widetilde{M}_S \\ \widetilde{N}_S \end{Bmatrix} + \begin{Bmatrix} \widetilde{L}_U \\ \widetilde{M}_U \\ \widetilde{N}_U \end{Bmatrix} + \begin{Bmatrix} \widetilde{L}_M \\ \widetilde{M}_M \\ \widetilde{N}_M \end{Bmatrix}. \tag{46}$$

The steady aerodynamic moments are computed for the projectile body with a cross product between the steady body aerodynamic force vector and the distance vector from the center of gravity to the center of pressure. Magnus moments on the body are computed in a similar way, with a cross product between the Magnus force vector and the distance vector from the center of gravity to the Magnus center of pressure. The unsteady body aerodynamic moments provide a damping source for projectile angular motion and are given by equation 47:

$$\begin{Bmatrix} \widetilde{L}_U \\ \widetilde{M}_U \\ \widetilde{N}_U \end{Bmatrix} = \widetilde{\gamma}_\alpha D \begin{Bmatrix} C_{DD} + \dfrac{\widetilde{p} D C_{LP}}{2V} \\ \dfrac{\widetilde{q} D C_{MQ}}{2V} \\ \dfrac{\widetilde{r} D C_{NR}}{2V} \end{Bmatrix}. \tag{47}$$

Air density is computed using the standard atmosphere (*13*).

4. Rotating Internal Part Projectile Linear Theory

The preceding equations of motion in their current state are highly nonlinear and while a solution, given an initial set of conditions, may be obtained numerically, it is desirable to solve them with a closed form solution for increased understanding of the dynamic behavior. Linear theory for symmetric rigid projectiles introduces a series of assumptions that yield a refined set of linear differential equations that can be solved in closed form. These equations form the basis of classic projectile stability theory. This same set of assumptions can be used to establish a linear theory for projectiles containing an axisymmetric rotating internal part in atmospheric flight. The necessary assumptions are as follows:

- The variable is changed from no-roll, station line velocity u, to total velocity V. Equations 48 and 49 relate V and u and their derivatives:

$$V = \sqrt{\widetilde{u}^2 + \widetilde{v}^2 + \widetilde{w}^2}\,; \tag{48}$$

$$\dot{V} = \left(\widetilde{u}\dot{\widetilde{u}} + \widetilde{v}\dot{\widetilde{v}} + \widetilde{w}\dot{\widetilde{w}}\right)/V\,. \tag{49}$$

- The variables are changed from time, *t*, to dimensionless arc length *s*. The dimensionless arc length, as defined by Murphy (*14*) is given in equation 50 and is measured in units of distance traveled:

$$s = \frac{1}{D}\int_0^t V d\tau\,. \tag{50}$$

Time and arc length derivatives of a dummy variable ζ are related by

$$\dot{\zeta} = (V/D)\zeta'\,; \tag{51}$$

$$\ddot{\zeta} = (V/D)^2(\zeta'' + \zeta' V'/V)\,. \tag{52}$$

- Euler yaw and pitch angles are small.

$$s_\theta \approx \theta \qquad c_\theta \approx 1 \qquad s_\psi \approx \psi \qquad c_\psi \approx 1\,. \tag{53}$$

- Aerodynamic angles of attack are small.

$$\alpha \approx \widetilde{w}/V \qquad \beta \approx \widetilde{v}/V\,. \tag{54}$$

- The effect of mass and inertia changes of a projectile on stability are well known. To properly evaluate the effects on stability solely due to the rotating internal part, the total mass of the two-component system is held constant and individual component mass and intertia properties are appropriately modified. This is accomplished by reevaluating the inertial properties of the projectile after the addition of the internal part based on its nominal characteristics prior to the addition of the internal part. Equation 55 provides the shift in the projectile's center of gravity due to the addition of the internal part, and equation 56 is used to populate the projectile's inertia matrix for various disk configurations.

$$\begin{Bmatrix} x_P \\ y_P \\ z_P \end{Bmatrix} = \frac{1}{m_P} \begin{Bmatrix} m_E x_E - m_D x_D \\ m_E y_E - m_D y_D \\ m_E z_E - m_D z_D \end{Bmatrix}; \tag{55}$$

$$I_P = I_E - m_P \begin{bmatrix} y_P^2 + z_P^2 & x_P y_P & x_P z_P \\ x_P y_P & x_P^2 + z_P^2 & y_P z_P \\ x_P z_P & y_P z_P & x_P^2 + y_P^2 \end{bmatrix} - T_D^T I_D T_D - m_D \begin{bmatrix} y_D^2 + z_D^2 & x_D y_D & x_D z_D \\ x_D y_D & x_D^2 + z_D^2 & y_D z_D \\ x_D z_D & y_D z_D & x_D^2 + y_D^2 \end{bmatrix}, \tag{56}$$

where

$$m_P = m_E - m_D\,. \tag{57}$$

- The projectile is aerodynamically symmetric.

$$C_{NR} = C_{MQ}\,. \tag{58}$$

$$C_{Y0} = C_{Z0} = 0\,. \tag{59}$$

$$C_{YB1} = C_{ZB1} = C_{NA}\,. \tag{60}$$

- A flat fire trajectory is assumed, and the force of gravity is neglected for stability analysis.
- The quantities V and ϕ are large compared to $\theta, \psi, \widetilde{q}, \widetilde{r}, \widetilde{v},$ and $\widetilde{w}$, such that products of small quantities and their derivatives are negligible.

After application of these assumptions, the differential equations can be solved in closed form as stated previously.

$$x' = D\,. \tag{61}$$

$$y' = (D/V)\widetilde{v} + \psi D\,. \tag{62}$$

$$z' = (D/V)\tilde{w} - \theta D \,. \tag{63}$$

$$\phi' = (D/V)\tilde{p} \,. \tag{64}$$

$$\theta' = (D/V)\tilde{q} \,. \tag{65}$$

$$\psi' = (D/V)\tilde{r} \,. \tag{66}$$

$$V' = -(\rho S D C_{X0} V)/2m_C \,. \tag{67}$$

$$p' = \left(\frac{\rho S D^2 (D C_{LP} \tilde{p} + 2 C_{DD} V)}{4(I_{DXX} + I_{PXX})} \right). \tag{68}$$

$$\begin{Bmatrix} v' \\ w' \\ q' \\ r' \end{Bmatrix} = \begin{bmatrix} A & 0 & 0 & -D \\ 0 & A & D & 0 \\ B & C & E & -F \\ -C & B & F & E \end{bmatrix} \begin{Bmatrix} \tilde{v} \\ \tilde{w} \\ \tilde{q} \\ \tilde{r} \end{Bmatrix}. \tag{69}$$

Equations 61–69 are linear, except for the total velocity, V, which is retained in several of the equations. It is assumed that V changes slowly with respect to the other state variables, and is considered to be constant where it appears in other dynamic equations. With this assumption, the total velocity, the angle of attack dynamics, and the roll dynamics all become uncoupled, linear-time invariant equations of motion.

Equation 69 is the matrix form of the epicyclic dynamic equations. The equations largely determine the angle-of-attack stability of the projectile. It should be noted that the basic structure of the epicyclic dynamic equations of a rigid projectile are the same as previously shown. Differences in the epicyclic dynamics of both configurations are contained in the coefficients B, C, E, and F. In the most general case, where the disk is located off the axis of symmetry and canted at an arbitrary angle, these coefficients are algebraically lengthy. While straightforward and computationally trivial to compute, space limitations here prevent the most general form of these coefficients to be listed. However, Appendix A provides these coefficients, as they would appear in the C-programming language. The symbolic form for the special case of the disk located on and aligned with the projectile axis of symmetry is also included in Appendix B.

The four roots of the characteristic equation shown in equation 69 are given in equation 70:

$$s = \left\{ \begin{matrix} \frac{1}{2}\left(A + E - iF \pm \sqrt{(A-E)^2 + 4CD - F^2 + 2i(AF - 2BD - EF)} \right) \\ \frac{1}{2}\left(A + E + iF \pm \sqrt{(A-E)^2 + 4CD - F^2 + 2i(EF + 2BD - AF)} \right) \end{matrix} \right\}. \tag{70}$$

These results are identical to conventional rigid projectile analysis. Consequently, rotating internal part projectile analysis can be approached in essentially the same manner that rigid projectiles are analyzed.

5. Example Results

In order to examine the changes an internal rotating disk induces on the dynamic behavior of a projectile, the following analysis documents how the fast and slow epicyclic modes change for various rotating disk arrangements. Results are shown for a typical 155-mm spin-stabilized artillery shell having a nominal weight of 94.88 lbf with a reference area of $S = 0.20$ ft^2 and a reference diameter of $D = 0.51$ ft. The nominal stationline, buttline, and waterline distances to the projectile's center of gravity are $x_E = 1.06$ ft, $y_E = 0.00$ ft, and $z_E = 0.00$ ft. The standard aerodynamic center of pressure and the aerodynamic center of Magnus are located at the following distances along the stationline, buttline, and waterline: $x_A = 1.76$ ft, $y_A = 0.00$ ft, $z_A = 0.00$ ft, and $x_M = 1.76$ ft, $y_M = 0.00$ ft, $z_M = 0.00$ ft. The moments of inertia about the body-axis are: $I_{EXX} = 0.11$ slug – ft^2, and $I_{EYY} = 1.40$ slug – ft^2, and $I_{EZZ} = 1.40$ slug – ft^2. The nominal disk is 0.33 ft in diameter, 0.06 ft thick, and weighs 9.5 lbf. It is nominally located on the projectile center of gravity and has the following inertia properties: $I_{DXX} = 0.0041$ slug – ft^2, $I_{DYY} = 0.0021$ slug – ft^2, and $I_{DZZ} = 0.0021$ slug – ft^2. Euler angles of the projectile are $\phi = 0.00$ rad, $\theta = 0.22$ rad, and $\psi = 0.00$ rad. The projectile has a forward velocity of $\tilde{u} = 2710$ ft/s and a spin rate of $\tilde{p} = 1674.10$ rad/s. The pitch and yaw rates and the side velocities are all equal to zero. The disk spin rate and angle are varied.

In the analysis to follow, the ratio of the disk mass to projectile mass is dubbed the mass ratio, M_R, the ratio of the disk spin rate to the projectile spin rate is called the spin ratio, S_R, and the angle that the disk spin axis is precessed from the projectile axis is given as the disk angle, ψ_D. The disk angle is defined in the inset of Figure 4 for a disk located off the projectile axis of symmetry in the buttline direction ($\bar{J}_B$ axis). A disk located on the projectile axis of symmetry can be visualized by setting the buttline offset distance equal to zero.

The effect on the epicyclic dynamics of the system of varying the disk angle for three different mass ratios with a spin ratio of 5 is demonstrated in the root-locus plots shown in Figures 4–6. The disk angle is varied from 0° (represented by the diamond) to 360°. The circle represents the eigenvalues for a disk angle of 90°, the square for a disk angle of 180°, and the bold **X** denotes the location of the eigenvalues determined from a similar rigid artillery round without a rotating internal part. These conventions are used for all root-locus plots. In Figures 4–8, the epicyclic modes travel from the diamond to the square as the disk angle is increased from 0° to 180°, and march back up the same path towards the diamond as the disk angle is further increased from 180° to 360°. In Figure 4 it can be seen that a disk of mass ratio 1/100 slightly affects the projectile fast and slow modes at angles other than 90°. Comparison of the three root-locus plots

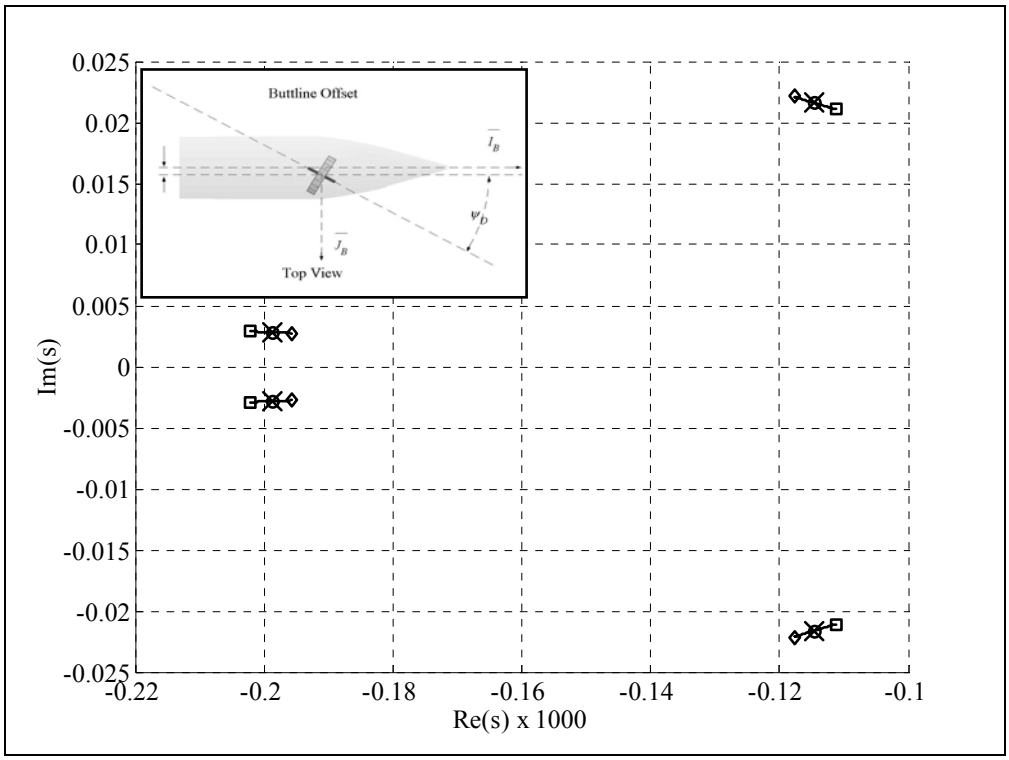

Figure 4. Root-locus for mass ratio = 1/100 and spin ratio = 5 (◊ = 0º, 360º disk angle; ○ = 90º disk angle; □ = 180º disk angle; x = rigid projectile).

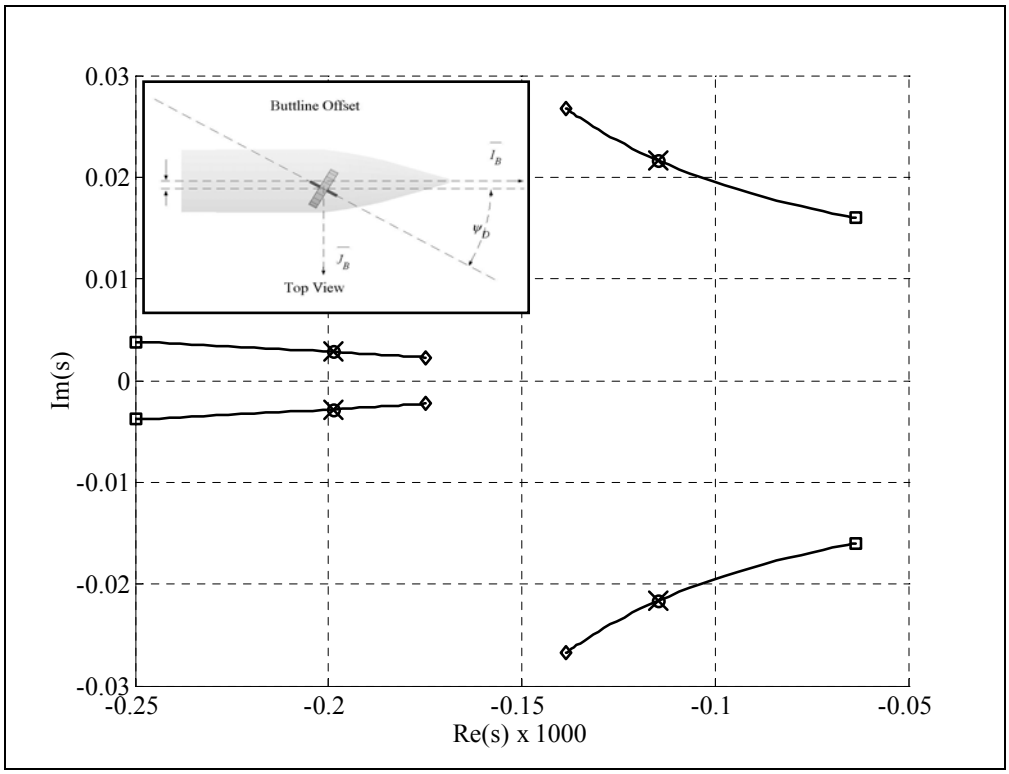

Figure 5. Root-locus for mass ratio = 1/10 and spin ratio = 5 (◊ = 0º, 360º disk angle; ○ = 90º disk angle; □ = 180º disk angle; x = rigid projectile).

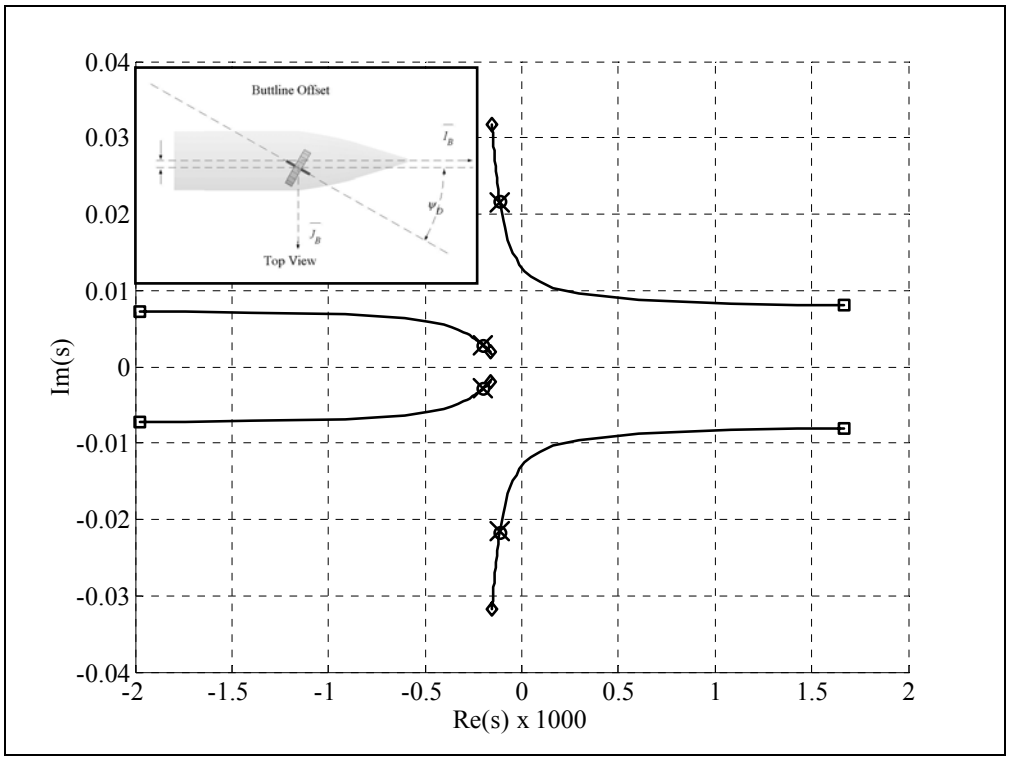

Figure 6. Root-locus for mass ratio = 1/5 and spin ratio = 5 (◊ = 0º, 360º disk angle; ○ = 90º disk angle; □ = 180º disk angle; x = rigid projectile).

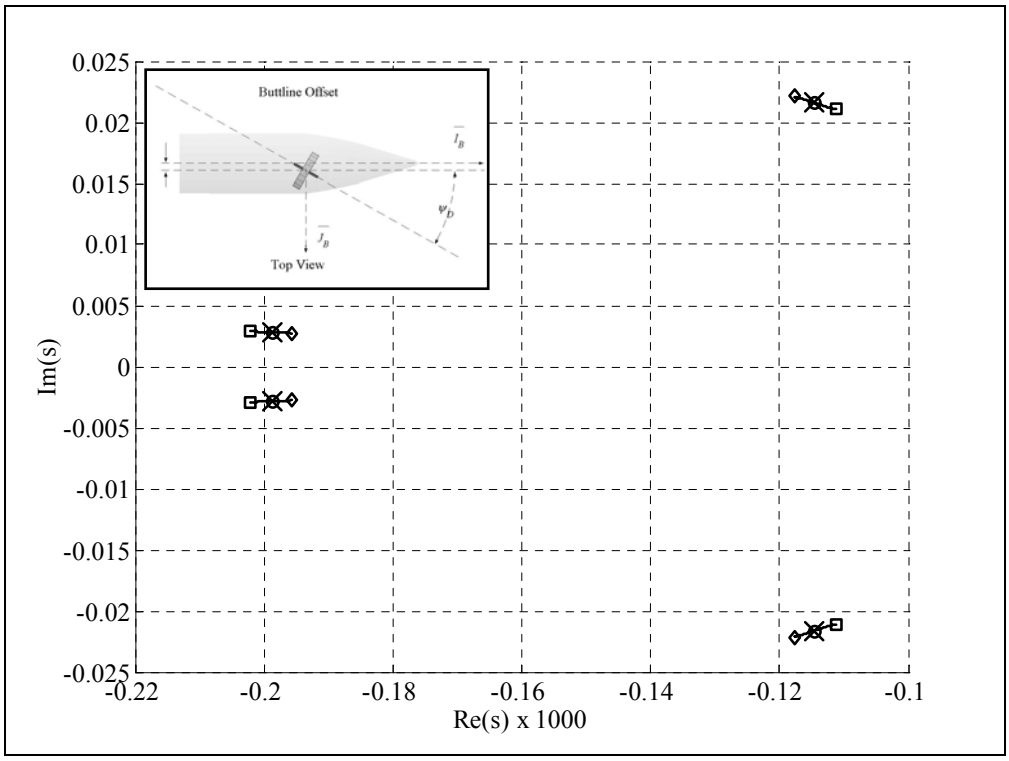

Figure 7. Root-locus for spin ratio = 1/2 and mass ratio = 1/10 (◊ = 0º, 360º disk angle; ○ = 90º disk angle; □ = 180º disk angle; x = rigid projectile).

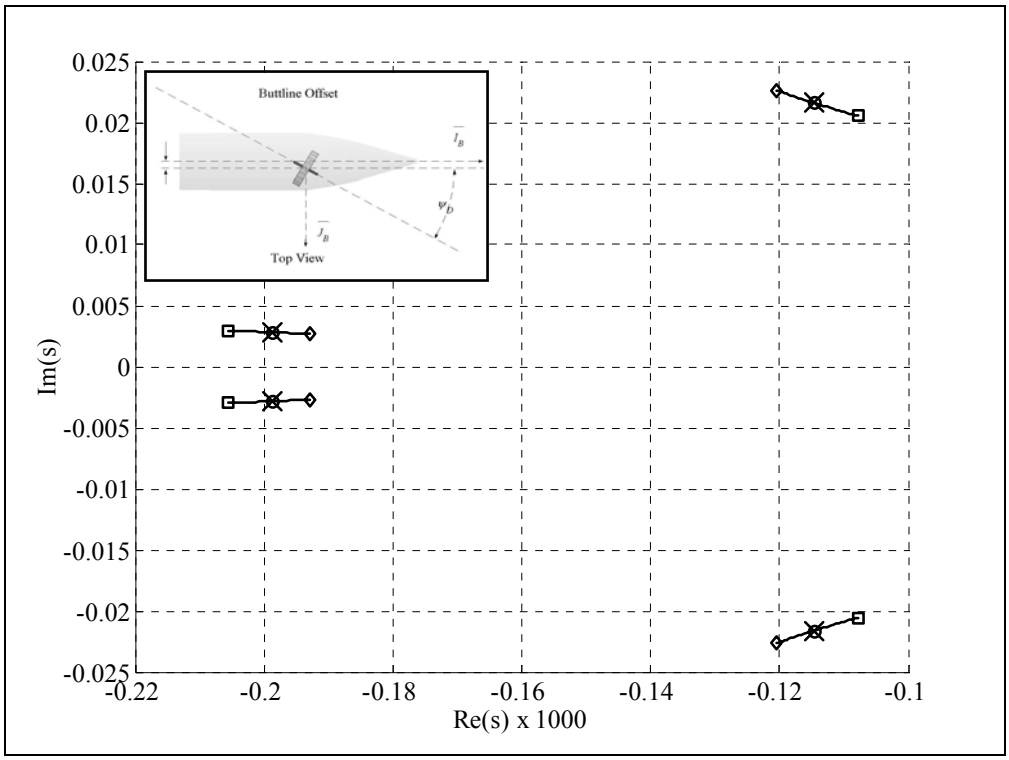

Figure 8. Root-locus for spin ratio = 1 and mass ratio = 1/10 (◊ = 0º, 360º disk angle; ○ = 90º disk angle; □ = 180º disk angle; x = rigid projectile).

reveals that increasing the mass ratio increases the effect that the spinning disk has on the epicyclic dynamics. As shown in Figure 6, when the mass ratio is sufficiently large, the fast mode can become unstable for large disk angles greater than 90°. In this case, spin stability of the complete round is adversely impacted by the component of disk angular velocity in the opposite direction of projectile spin. Also note that the mass ratio has very little effect on the stability of the system for a disk angle of 90°. For disk angles >180°, the eigenvalues march back along the same path toward 0°. This is expected because for a disk located on the projectile axis of symmetry the disk angles from 0° to 180° relative to the projectile are equivalent to the angles from 180° to 360° with the direction of spin reversed.

Figures 7–9 are the root-locus plots obtained by varying the disk angle for three different spin ratios with a disk to projectile mass ratio of 1/10. By comparing Figures 7–9, it is shown that decreasing spin ratio diminishes the effect that a spinning disk of a given mass has on the epicyclic modes. The opposite holds true as well. Increasing the spin ratio increases the dynamic effects and is capable of driving the system unstable for certain disk angles. Comparison of Figures 6 and 9 shows that the same dynamic effects can be achieved with either mass ratio or spin ratio. Figures 4–9 also demonstrate that a disk of any mass ratio, spinning in the same direction as the projectile (i.e., disk angle <90°), tends to stabilize the fast mode of the system while destabilizing the slow mode. Disk angles of >90° up to 180° have the opposite effect. However, for large spin ratios and large mass ratios, the movement of the modes is much

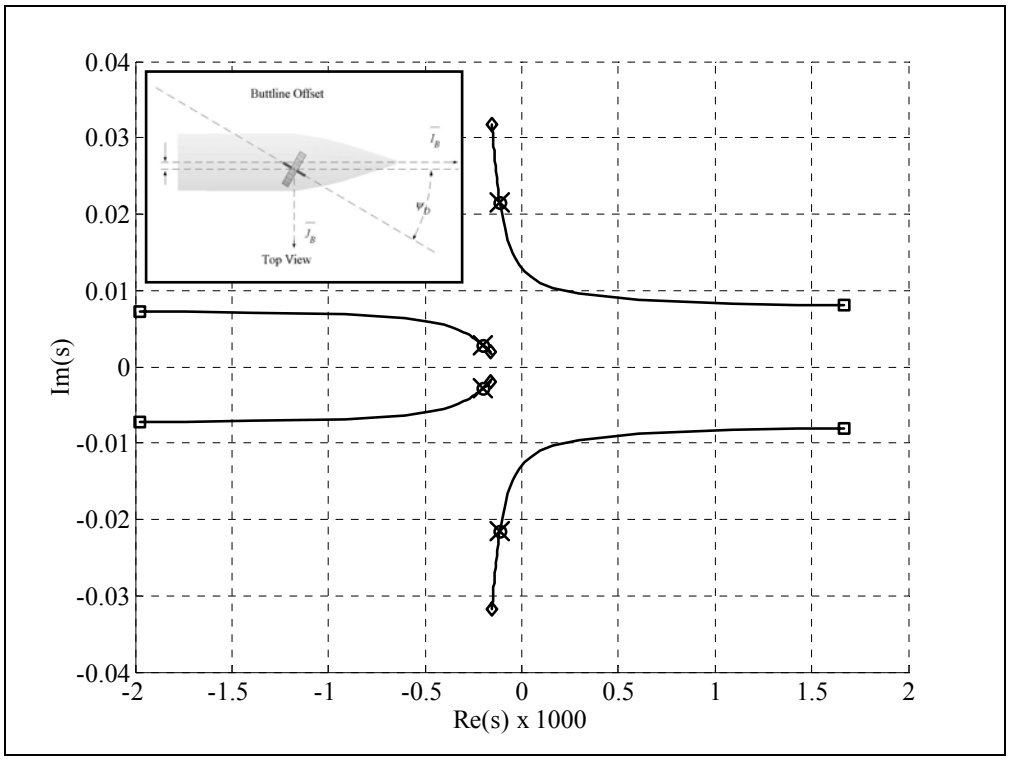

Figure 9. Root-locus for spin ratio = 10 and mass ratio = 1/10 (◊ = 0º, 360º disk angle; ○ = 90º disk angle; □ = 180º disk angle; x = rigid projectile).

greater per increase in disk angle. While not explicitly shown previously, stationline position of the disk has no effect on the fast and slow modes when the disk mass center is located on the projectile axis of symmetry. Moreover, in this case, if the product $M_R S_R$ is held constant, the fast and slow modes do not change with disk location along the projectile axis of symmetry.

Figures 9 and 10 examine the fast and slow modes for spinning disks that are located off the projectile axis of symmetry in the buttline direction and the waterline direction. It is important to make this distinction because rotating the disk about the $\vec{K}_B$ axis from the projectile axis of symmetry produces two unique angles relative to the projectile in each direction. Analysis of the fast and slow modes for a system with the disk located off the projectile axis of symmetry in the buttline direction and varying its position in the direction of the stationline produce the same mode path as that for a disk located on the projectile axis of symmetry and varying its stationline location. The path is the same, however, the locations of the modes along the path do vary slightly with stationline position. This slight variation is undetectable on the scale used for graphs shown in this report. Therefore, Figure 9 can be referred to for a root-locus of the previously mentioned system for a disk located anywhere along the stationline and anywhere off the axis in the buttline direction. The stationline location does, however, change the fast and slow modes of the system for a disk that is located off-axis in the waterline direction as shown in Figure 10.

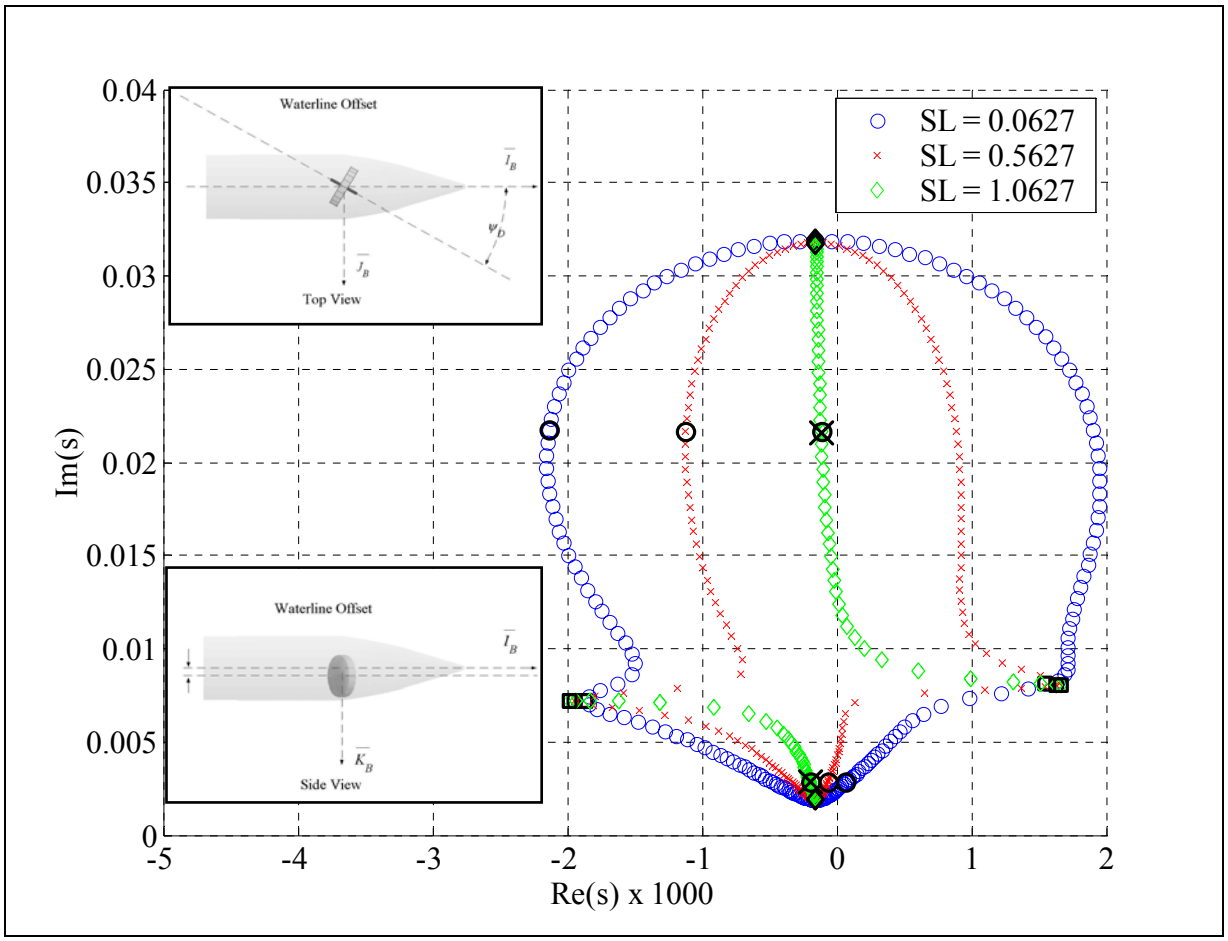

Figure 10. Root-locus for a disk located 3/4 in off-axis of symmetry in the waterline direction (spin ratio = 10, mass ratio = 1/10) (◊ = 0º, 360º disk angle; ○ = 90º disk angle; □ = 180º disk angle; x = rigid projectile).

In Figure 10, the fast and slow modes are plotted in increments of disk angle, and to add clarity to the graphs only the eigenvalues containing positive imaginary parts are shown. The root-locus for the stationline of the disk center of gravity that coincides with the stationline of the projectile center of gravity is the same as that for disks either located on the axis of symmetry or off-axis in the buttline direction. The plots are only shown for stationline positions varied from the aft of the projectile to its center of gravity. Disks that are located forward of the projectile center of gravity, at distances from the center of gravity equal to those that are aft of it, produce the same modes for the respective distances. Notice that the fast modes for SL = 0.0627 ft and SL = 0.5627 ft become slow modes at a disk angle of 180° (designated by the square) and the slow modes change to fast modes. It is also interesting that for these two curves the directions of the root-locus path change for disk angles slightly <180° and slightly >90° (designated by the circle). The previously mentioned studies show that for a disk located at the projectile center of gravity stationline, the epicyclic dynamics of the system are not affected by the off-axis disk location. They also show that a spinning disk mounted at an angle of 90° with a stationline position equal to the stationline of the center of gravity of the projectile is the same system as a

rigid projectile without a disk. The slow mode of the system with a disk located off-axis in the buttline direction is predominantly on the left side of the s-plane, whereas for a disk located off-axis in the direction of the waterline the slow mode is divided between the left and right sides of the s-plane.

Figures 11 and 12 show the root-locus for various angles of a disk located off-axis in various directions lying between the waterline and buttline. The fast mode shown in Figure 11 and the slow mode in Figure 12 are for a disk located 1/4 in off the projectile axis of symmetry with a spin ratio of 10 and mass ratio of 1/10 mounted at 0.0627 ft along the stationline. The lines running vertically represent the epicyclic mode locations for different directions of offset defined in the figure legend. The center of gravity location is the same regardless of the disk angle. The vertical line running roughly down the center of the plot represents the epicyclic modes for a disk located solely in the positive buttline direction. Each horizontal line in the graph represents the epicyclic mode locations for a specific disk angle designated by the values shown. The horizontal lines located on the left-hand side of the center line represent angles from 0° to 180°, and those on the right-hand side represent angles from 180° to 360°. If the fast mode of a disk spinning at an angle of 120° and located 45° from the positive buttline direction were desired to be known, one would follow the dash-dot line until it crossed the bottom half of the 120° curve and arrive at a value of $-0.53E^{-3}+0.017i$. These plots definitively show that the epicyclic modes of a projectile containing a rotating internal part are significantly affected by the location and angle of the rotating internal part. Figure 13 shows a system with a disk mounted at 0.0627 ft along the stationline and at various distances off-axis in a direction equidistant from the buttline and waterline. Increasing the distance that the disk is located off-axis increases the effects that the spinning disk has on the dynamics of the system. Greater distances off-axis cause the fast and slow modes to swap at disk angles near 180°, whereas smaller distances, such as 1/4 in, shown in Figures 11 and 12, do not. Figure 14 shows the root-locus for a disk located 3/4 in off the projectile axis of symmetry in a direction equidistant from the waterline and buttline directions for various spin ratios. Like disks located on the axis of symmetry, increasing the spin ratio increases the range of the epicyclic modes. For disk angles between 0° and 180° the fast mode is predominantly on the left-hand side of the imaginary axis, and the slow mode is predominantly on the right-hand side. The opposite is true for disk angles between 180° and 360°. Increasing the spin ratio moves the modes farther from the imaginary axis for disk angles other than 0° and 360° and expands their range along the imaginary axis.

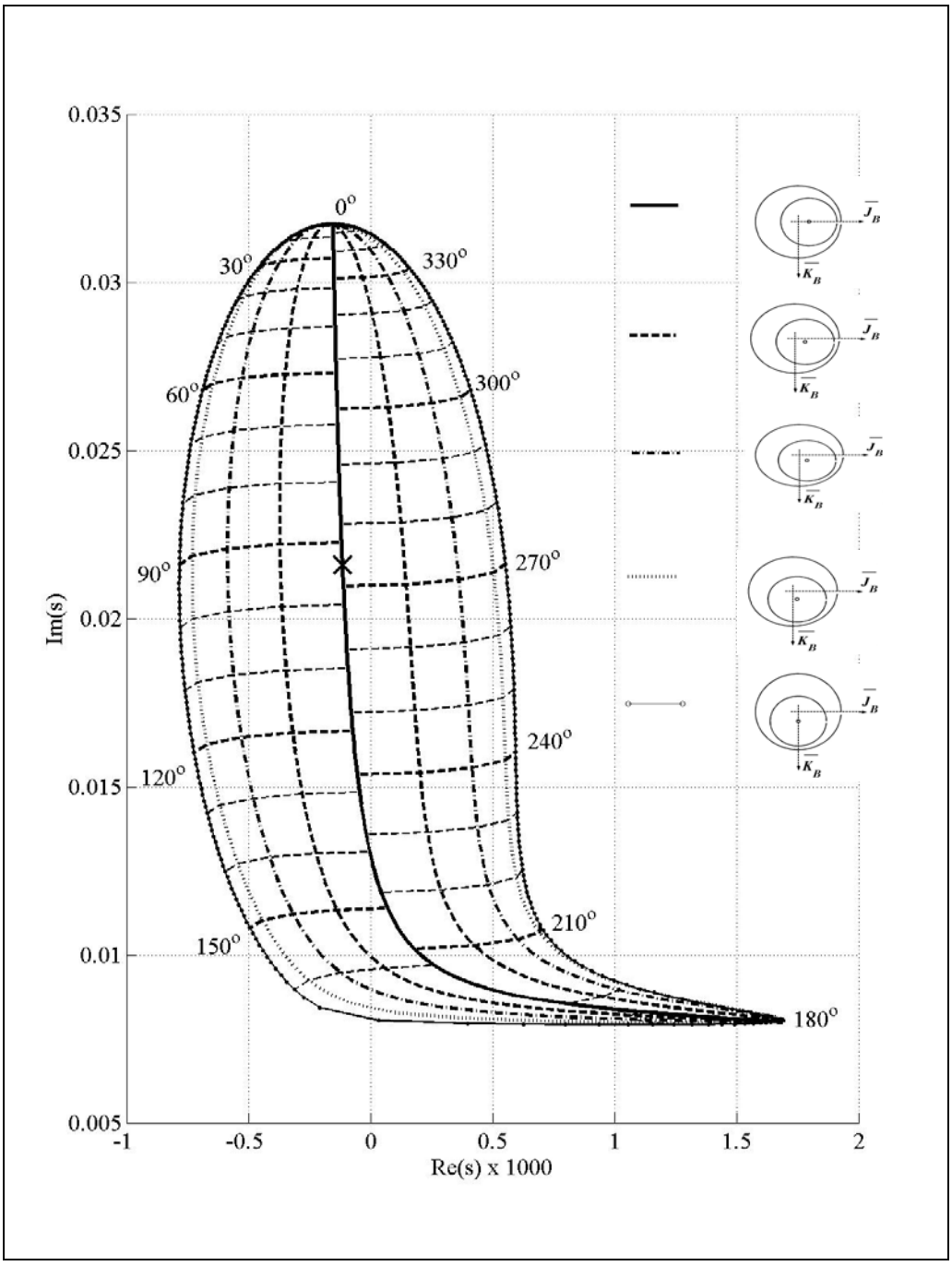

Figure 11. Fast mode root-locus for a disk located 1/4 in off-axis of symmetry in the waterline and buttline directions (spin ratio = 10; mass ratio = 1/10).

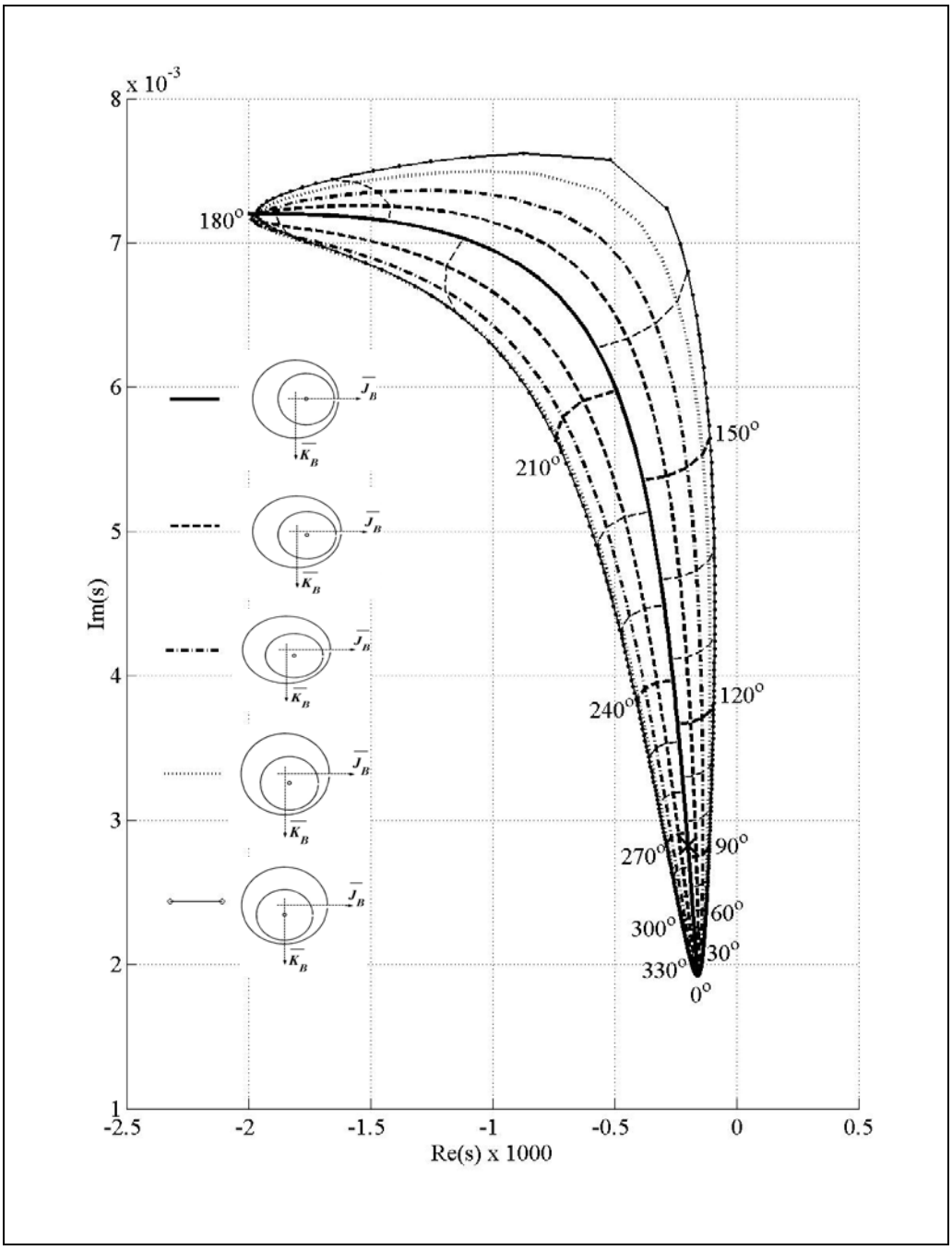

Figure 12. Slow mode root-locus for a disk located 1/4 in off-axis of symmetry in the waterline and buttline directions (spin ratio = 10; mass ratio = 1/10).

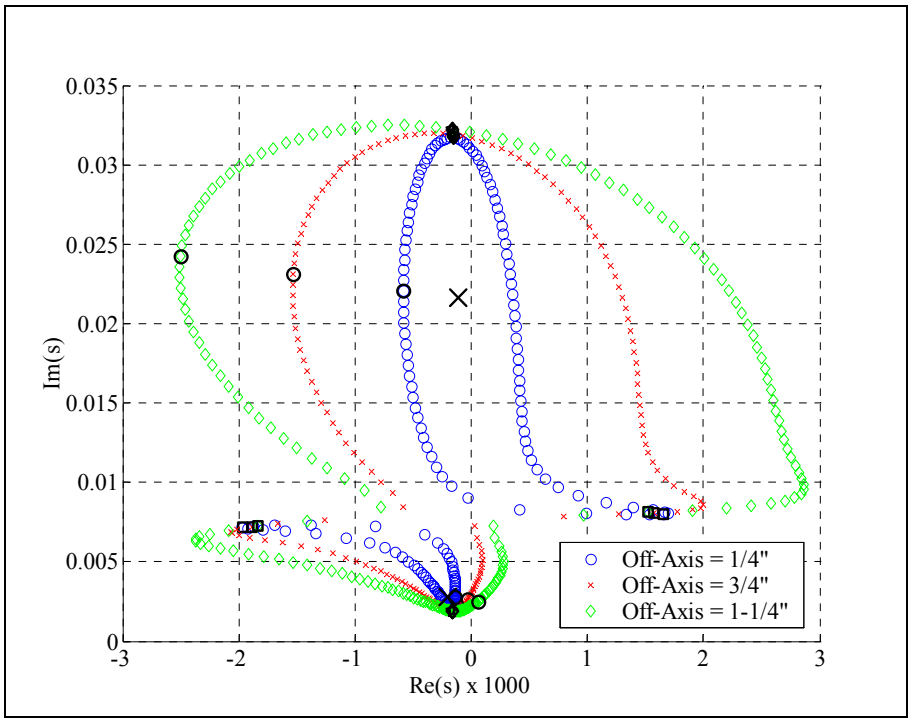

Figure 13. Root-locus for a disk located at various distances off-axis of symmetry in a direction equidistant from the waterline and buttline directions (spin ratio = 10; mass ratio = 1/10) (◊ = 0º, 360º disk angle; ○ = 90º disk angle; □ = 180º disk angle; x = rigid projectile).

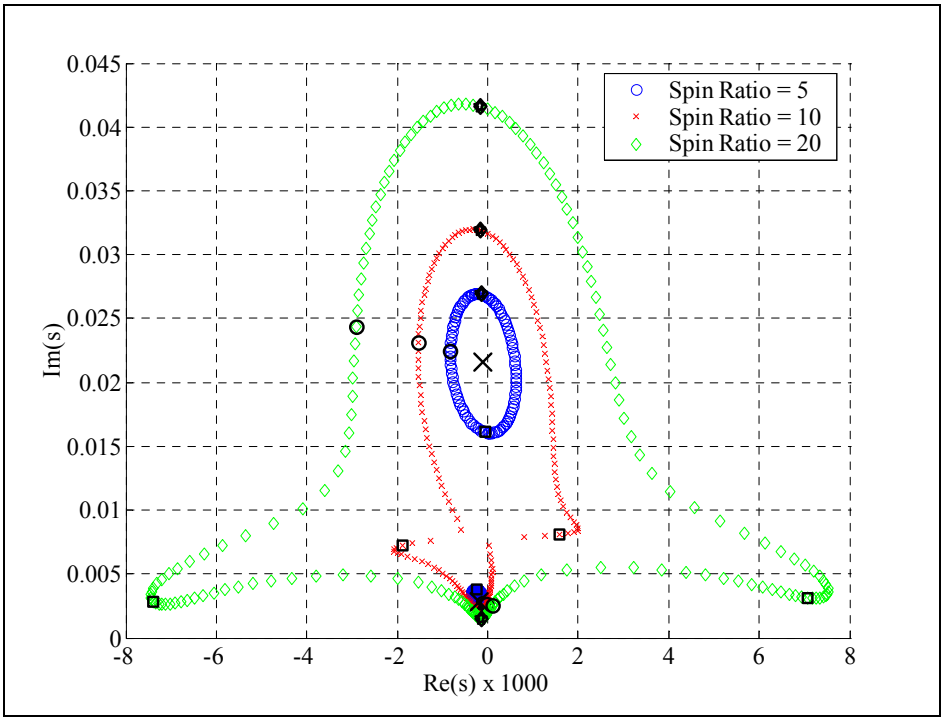

Figure 14. Root-locus for a disk located 3/4 in off-axis of symmetry in a direction equidistant from the waterline and buttline directions for various spin ratios (mass ratio = 1/10) (◊ = 0º, 360º disk angle; ○ = 90º disk angle; □ = 180º disk angle; x = rigid projectile).

6. Conclusions

The equations of motion for a projectile containing an axisymmetric rotating internal disk that spins at a constant rate have been developed. The model allows for the disk to be located off the axis of symmetry of the projectile and oriented at an arbitrary angle relative to the projectile axis of symmetry. Projectile linear theory has been modified to accommodate projectile configurations that contain an internal rotating disk. The addition of an internal rotating disk alters several of the coefficients in the epicyclic dynamic equations leading to modified fast and slow epicyclic modes.Using modified projectile linear theory, the effect of disk mass, speed, and location is systematically studied. If the mass ratio times the spin ratio is held constant the same epicyclic modes are produced for a disk located at any position along the projectile axis of symmetry. For a specified mass and spin ratio the stationline position of the disk has no effect on the dynamics of the system for a disk located either on the projectile axis of symmetry. However, the stationline position does affect the dynamics if the disk is off-axis. In these instances, the farther the disk is located away from the center of gravity of the projectile the more influence its mass, spin rate, and angle relative to the projectile axis of symmetry have on the epicyclic dynamics of the system.

7. References

1. Murphy, C. Symmetric Missile Dynamic Instabilities. *Journal of Guidance and Control* **1981,** *4* (5), 464–471.

2. Soper, W. Projectile Instability Produced by Internal Friction. *AIAA Journal* **1978**, *16* (1), 8–11.

3. Murphy, C. Influence of Moving Internal Parts on Angular Motion of Spinning Projectiles. *Journal of Guidance and Control* **1978**, *1* (2), 117–122.

4. D'Amico, W. Comparison of Theory and Experiment for Moments Induced by Loose Internal Parts. *Journal of Guidance and Control* **1987**, *10* (1), 14–19.

5. Hodapp, A. Passive Means for Stabilizing Projectiles With Partially Restrained Internal Members. *Journal of Guidance and Control* **1989**, *12* (2), 135–139.

6. Goddard, R. Apparatus for Steering Aircraft. U.S. Patent 2,594,766, April 1952.

7. Barrett, R.; Stutts, J. *Modeling, Design, and Testing of a Barrel-Launched Adaptive Munition*. Proceedings of the 4th Annual Society of Photo-Optical Engineers Symposium on Smart Structures, San Diego, CA; Society of Photo-Optical Engineers: New York, March 1997.

8. Schmidt, E.; Donovan, V. Technique to Reduce Yaw and Jump of Fin-Stabilized Projectiles. *Journal of Spacecraft and Rockets* **1998**, *35* (1), 110–111.

9. Costello, M.; Agarwalla, R. Improved Dispersion of a Fin Stabilized Projectile Using a Passive Moveable Nose. *Journal of Guidance, Control, and Dynamics* **2000**, *23* (5), 900–903.

10. Smith, J.; Smith, K.; Topliffe, R. *Feasibility Study for Application of Modular Guidance and Control Units to Existing ICM Projectiles*; ARLCD-CR-79001; U.S. Army Armament Research and Development Command: Picatinny Arsenal, Dover, NJ, 1978.

11. Costello, M.; Peterson, A. Linear Theory of a Dual Spin Projectile in Atmospheric Flight. *Journal of Guidance, Control, and Dynamics* **2000**, *23* (4), 789–797.

12. Burchett, B.; Peterson, A.; Costello, M. Prediction of Swerving Motion of a Dual-Spin Projectile With Lateral Pulse Jets in Atmospheric Flight. *Mathematical and Computer Modeling* **2002**, *35* (7–8), 821–834.

13. Von Mises, R. *Theory of Flight*. Dover: New York, 1959; Chapter 1.

14. Murphy, C. H. *Free Flight Motion of Symmetric Missiles*; Report 1216; U.S. Army Ballistic Research Laboratory: Aberdeen Proving Ground, MD, 1963.

Appendix A. Coefficients of the Epicyclic Dynamic Equations in C-Form

This appendix appears in its original form, without editorial change.

The coefficients of the characteristic equation in C-programming language form are given in equations A1–A6. The equations were derived using Wolfram Research Inc.'s Mathematica and the following variable substitutions need to be made in order for their appearance to be consistent with the text.

Variable Substitutions

dx,dy, dz $\Leftrightarrow x_{PD}, y_{PD}, z_{PD}$	dax, day, daz $\Leftrightarrow x_{PA}, y_{PA}, z_{PA}$	dmx, dmy, dmz $\Leftrightarrow x_{PM}, y_{PM}, z_{PM}$
phi, theta, psi $\Leftrightarrow \phi, \theta, \psi$	md $\Leftrightarrow m_D$	mp $\Leftrightarrow m_P$
CYPA $\Leftrightarrow C_{YPA}$	CNA $\Leftrightarrow C_{NA}$	CMQ $\Leftrightarrow C_{MQ}$
CLP $\Leftrightarrow C_{LP}$	CDD $\Leftrightarrow C_{DD}$	CX0, CY0, CZ0 $\Leftrightarrow C_{X0}, C_{Y0}, C_{Z0}$
CX2 $\Leftrightarrow C_{X2}$	CYB1, CZB1 $\Leftrightarrow C_{YB1}, C_{ZB1}$	rho $\Leftrightarrow \rho$
omega $\Leftrightarrow \Omega$	Cos(disk), Sin(disk), $0 \Leftrightarrow n_X, n_Y, n_Z$	

JPXX, JPYY, JPZZ, JPXY, JPXZ, JPYZ $\Leftrightarrow I_{PXX}, I_{PYY}, I_{PZZ}, I_{PXY}, I_{PXZ}, I_{PYZ}$

JDXX, JDYY, JDZZ, JDXY, JDXZ, JDYZ $\Leftrightarrow I_{DXX}, I_{DYY}, I_{DZZ}, I_{DXY}, I_{DXZ}, I_{DYZ}$

A1) $A =$ -(CNA*D*rho*S)/(2.*mc)

A2) $B =$ (D*(-((-((Cos(phi)*(JPXY - (dx*dy*md*mp)/(md + mp) + (JDXX - &
JDYY)*Cos(disk)*Sin(disk)) + (-JPXZ + (dx*dz*md*mp)/(md + &
mp))*Sin(phi))*(-(CYPA*D*dy*md*pt*rho*S*Cos(phi))/(4.*(md + mp)) + &
(CNA*dz*md*rho*S*V*Cos(phi))/(2.*(md + mp)) + &
(CYPA*D*dz*md*pt*rho*S*Sin(phi))/(4.*(md + mp)) + &
(CNA*dy*md*rho*S*V*Sin(phi))/(2.*(md + mp)))) + (JPXX + ((Power(dy,2) + &
Power(dz,2))*md*mp)/(md + mp) + JDXX*Power(Cos(disk),2) + &
JDYY*Power(Sin(disk),2))*(-(CYPA*D*dmx*pt*rho*S)/4. + &
(CYPA*D*dx*md*pt*rho*S*Power(Cos(phi),2))/(4.*(md + mp)) + &
(CYPA*D*dx*md*pt*rho*S*Power(Sin(phi),2))/(4.*(md + &
mp))))/(-Power(Cos(phi)*(JPXY - (dx*dy*md*mp)/(md + mp) + (JDXX - &
JDYY)*Cos(disk)*Sin(disk)) + (-JPXZ + (dx*dz*md*mp)/(md + mp))*Sin(phi),2)
+ &
((JPXX + ((Power(dy,2) + Power(dz,2))*md*mp)/(md + mp) + &
JDXX*Power(Cos(disk),2) + &
JDYY*Power(Sin(disk),2))*(Power(Cos(phi),2)*(JPYY*md + JPYY*mp + &
Power(dx,2)*md*mp + Power(dz,2)*md*mp + JDYY*(md +
mp)*Power(Cos(disk),2) + &
JDXX*(md + mp)*Power(Sin(disk),2)) + Sin(phi)*(2*dy*dz*md*mp*Cos(phi) +
&
((Power(dx,2) + Power(dy,2))*md*mp + JDYY*(md + mp) + JPYY*(md + &

```
mp))*Sin(phi)) - JPYZ*(md + mp)*Sin(2*phi)))/(md + mp))) +  &
((-((Cos(phi)*(JPXY - (dx*dy*md*mp)/(md + mp) + (JDXX -  &
JDYY)*Cos(disk)*Sin(disk)) + (-JPXZ + (dx*dz*md*mp)/(md +  &
mp))*Sin(phi))*((JPXZ - (dx*dz*md*mp)/(md + mp))*Cos(phi) + (JPXY -  &
(dx*dy*md*mp)/(md + mp) + (JDXX - JDYY)*Cos(disk)*Sin(disk))*Sin(phi))) +
&
((JPXX + ((Power(dy,2) + Power(dz,2))*md*mp)/(md + mp) +  &
JDXX*Power(Cos(disk),2) + JDYY*Power(Sin(disk),2))*((-(dy*dz*md*mp) +  &
JPYZ*(md + mp))*Power(Cos(phi),2) + Cos(phi)*(-(JDYY*md) - JDYY*mp -  &
Power(dy,2)*md*mp + Power(dz,2)*md*mp + JDYY*(md +
mp)*Power(Cos(disk),2) +  &
JDXX*(md + mp)*Power(Sin(disk),2))*Sin(phi) - (-(dy*dz*md*mp) + JPYZ*(md
+  &
mp))*Power(Sin(phi),2)))/(md + mp))*(-((-((Cos(phi)*(JPXY -
(dx*dy*md*mp)/(md  &
+ mp) + (JDXX - JDYY)*Cos(disk)*Sin(disk)) + (-JPXZ + (dx*dz*md*mp)/(md
+  &
mp))*Sin(phi))*((JPXZ - (dx*dz*md*mp)/(md + mp))*Cos(phi) + (JPXY -  &
(dx*dy*md*mp)/(md + mp) + (JDXX - JDYY)*Cos(disk)*Sin(disk))*Sin(phi))) +
&
((JPXX + ((Power(dy,2) + Power(dz,2))*md*mp)/(md + mp) +  &
JDXX*Power(Cos(disk),2) + JDYY*Power(Sin(disk),2))*((-(dy*dz*md*mp) +  &
JPYZ*(md + mp))*Power(Cos(phi),2) + Cos(phi)*(-(JDYY*md) - JDYY*mp -  &
Power(dy,2)*md*mp + Power(dz,2)*md*mp + JDYY*(md +
mp)*Power(Cos(disk),2) +  &
JDXX*(md + mp)*Power(Sin(disk),2))*Sin(phi) - (-(dy*dz*md*mp) + JPYZ*(md
+  &
mp))*Power(Sin(phi),2)))/(md + mp))*(-((Cos(phi)*(JPXY - (dx*dy*md*mp)/(md
+  &
mp) + (JDXX - JDYY)*Cos(disk)*Sin(disk)) + (-JPXZ + (dx*dz*md*mp)/(md +
&
mp))*Sin(phi))*(-(CYPA*D*dy*md*pt*rho*S*Cos(phi))/(4.*(md + mp)) +  &
(CNA*dz*md*rho*S*V*Cos(phi))/(2.*(md + mp)) +  &
(CYPA*D*dz*md*pt*rho*S*Sin(phi))/(4.*(md + mp)) +  &
(CNA*dy*md*rho*S*V*Sin(phi))/(2.*(md + mp)))) + (JPXX + ((Power(dy,2) +
&
Power(dz,2))*md*mp)/(md + mp) + JDXX*Power(Cos(disk),2) +  &
JDYY*Power(Sin(disk),2))*(-(CYPA*D*dmx*pt*rho*S)/4. +  &
(CYPA*D*dx*md*pt*rho*S*Power(Cos(phi),2))/(4.*(md + mp)) +  &
(CYPA*D*dx*md*pt*rho*S*Power(Sin(phi),2))/(4.*(md + mp))))) +  &
(-((-(CYPA*D*dy*md*pt*rho*S*Cos(phi))/(4.*(md + mp)) +  &
(CNA*dz*md*rho*S*V*Cos(phi))/(2.*(md + mp)) +  &
(CYPA*D*dz*md*pt*rho*S*Sin(phi))/(4.*(md + mp)) +  &
(CNA*dy*md*rho*S*V*Sin(phi))/(2.*(md + mp)))*((JPXZ -
(dx*dz*md*mp)/(md +  &
mp))*Cos(phi) + (JPXY - (dx*dy*md*mp)/(md + mp) + (JDXX -  &
```

```
JDYY)*Cos(disk)*Sin(disk))*Sin(phi))) + (JPXX + ((Power(dy,2) +  &
Power(dz,2))*md*mp)/(md + mp) + JDXX*Power(Cos(disk),2) +  &
JDYY*Power(Sin(disk),2))*((CNA*dax*rho*S*V)/2. -  &
(CNA*dx*md*rho*S*V*Power(Cos(phi),2))/(2.*(md + mp)) -  &
(CNA*dx*md*rho*S*V*Power(Sin(phi),2))/(2.*(md + mp))))*(-
Power(Cos(phi)*(JPXY  &
- (dx*dy*md*mp)/(md + mp) + (JDXX - JDYY)*Cos(disk)*Sin(disk)) + (-JPXZ +
&
(dx*dz*md*mp)/(md + mp))*Sin(phi),2) + ((JPXX + ((Power(dy,2) +  &
Power(dz,2))*md*mp)/(md + mp) + JDXX*Power(Cos(disk),2) +  &
JDYY*Power(Sin(disk),2))*(Power(Cos(phi),2)*(JPYY*md + JPYY*mp +  &
Power(dx,2)*md*mp + Power(dz,2)*md*mp + JDYY*(md +
mp)*Power(Cos(disk),2) +  &
JDXX*(md + mp)*Power(Sin(disk),2)) + Sin(phi)*(2*dy*dz*md*mp*Cos(phi) +
&
((Power(dx,2) + Power(dy,2))*md*mp + JDYY*(md + mp) + JPYY*(md +  &
mp))*Sin(phi)) - JPYZ*(md + mp)*Sin(2*phi)))/(md +  &
mp))))/((-Power(Cos(phi)*(JPXY - (dx*dy*md*mp)/(md + mp) + (JDXX -  &
JDYY)*Cos(disk)*Sin(disk)) + (-JPXZ + (dx*dz*md*mp)/(md + mp))*Sin(phi),2)
+  &
((JPXX + ((Power(dy,2) + Power(dz,2))*md*mp)/(md + mp) +  &
JDXX*Power(Cos(disk),2) +  &
JDYY*Power(Sin(disk),2))*(Power(Cos(phi),2)*(JPYY*md + JPYY*mp +  &
Power(dx,2)*md*mp + Power(dz,2)*md*mp + JDYY*(md +
mp)*Power(Cos(disk),2) +  &
JDXX*(md + mp)*Power(Sin(disk),2)) + Sin(phi)*(2*dy*dz*md*mp*Cos(phi) +
&
((Power(dx,2) + Power(dy,2))*md*mp + JDYY*(md + mp) + JPYY*(md +  &
mp))*Sin(phi)) - JPYZ*(md + mp)*Sin(2*phi)))/(md +  &
mp))*(-Power(-((Cos(phi)*(JPXY - (dx*dy*md*mp)/(md + mp) + (JDXX -  &
JDYY)*Cos(disk)*Sin(disk)) + (-JPXZ + (dx*dz*md*mp)/(md +  &
mp))*Sin(phi))*((JPXZ - (dx*dz*md*mp)/(md + mp))*Cos(phi) + (JPXY -  &
(dx*dy*md*mp)/(md + mp) + (JDXX - JDYY)*Cos(disk)*Sin(disk))*Sin(phi))) +
&
((JPXX + ((Power(dy,2) + Power(dz,2))*md*mp)/(md + mp) +  &
JDXX*Power(Cos(disk),2) + JDYY*Power(Sin(disk),2))*((-(dy*dz*md*mp) +  &
JPYZ*(md + mp))*Power(Cos(phi),2) + Cos(phi)*(-(JDYY*md) - JDYY*mp -  &
Power(dy,2)*md*mp + Power(dz,2)*md*mp + JDYY*(md +
mp)*Power(Cos(disk),2) +  &
JDXX*(md + mp)*Power(Sin(disk),2))*Sin(phi) - (-(dy*dz*md*mp) + JPYZ*(md
+  &
mp))*Power(Sin(phi),2)))/(md + mp),2) + (-Power(Cos(phi)*(JPXY -  &
(dx*dy*md*mp)/(md + mp) + (JDXX - JDYY)*Cos(disk)*Sin(disk)) + (-JPXZ +
&
(dx*dz*md*mp)/(md + mp))*Sin(phi),2) + ((JPXX + ((Power(dy,2) +  &
Power(dz,2))*md*mp)/(md + mp) + JDXX*Power(Cos(disk),2) +  &
```

```
JDYY*Power(Sin(disk),2))*(Power(Cos(phi),2)*(JPYY*md + JPYY*mp +  &
Power(dx,2)*md*mp + Power(dz,2)*md*mp + JDYY*(md +
mp)*Power(Cos(disk),2) +  &
JDXX*(md + mp)*Power(Sin(disk),2)) + Sin(phi)*(2*dy*dz*md*mp*Cos(phi) +
&
((Power(dx,2) + Power(dy,2))*md*mp + JDYY*(md + mp) + JPYY*(md +  &
mp))*Sin(phi)) - JPYZ*(md + mp)*Sin(2*phi)))/(md + mp))*(-Power((JPXZ -  &
(dx*dz*md*mp)/(md + mp))*Cos(phi) + (JPXY - (dx*dy*md*mp)/(md + mp) +
(JDXX -  &
JDYY)*Cos(disk)*Sin(disk))*Sin(phi),2) + ((JPXX + ((Power(dy,2) +  &
Power(dz,2))*md*mp)/(md + mp) + JDXX*Power(Cos(disk),2) +  &
JDYY*Power(Sin(disk),2))*(((Power(dx,2) + Power(dy,2))*md*mp + JDYY*(md
+ mp)  &
+ JPYY*(md + mp))*Power(Cos(phi),2) - 2*dy*dz*md*mp*Cos(phi)*Sin(phi) +
&
(JPYY*md + JPYY*mp + Power(dx,2)*md*mp + Power(dz,2)*md*mp +
JDYY*(md +  &
mp)*Power(Cos(disk),2) + JDXX*(md +
mp)*Power(Sin(disk),2))*Power(Sin(phi),2)  &
+ JPYZ*(md + mp)*Sin(2*phi)))/(md + mp))))))/V
```

A3) $C =$

```
(D*(-((-((Cos(phi)*(JPXY - (dx*dy*md*mp)/(md + mp) + (JDXX -  &
JDYY)*Cos(disk)*Sin(disk)) + (-JPXZ + (dx*dz*md*mp)/(md +  &
mp))*Sin(phi))*(-(CYPA*D*dz*md*pt*rho*S*Cos(phi))/(4.*(md + mp)) -  &
(CNA*dy*md*rho*S*V*Cos(phi))/(2.*(md + mp)) -  &
(CYPA*D*dy*md*pt*rho*S*Sin(phi))/(4.*(md + mp)) +  &
(CNA*dz*md*rho*S*V*Sin(phi))/(2.*(md + mp)))) + (JPXX + ((Power(dy,2) +
&
Power(dz,2))*md*mp)/(md + mp) + JDXX*Power(Cos(disk),2) +  &
JDYY*Power(Sin(disk),2))*(-(CNA*dax*rho*S*V)/2. +  &
(CNA*dx*md*rho*S*V*Power(Cos(phi),2))/(2.*(md + mp)) +  &
(CNA*dx*md*rho*S*V*Power(Sin(phi),2))/(2.*(md + mp))))/(-
Power(Cos(phi)*(JPXY  &
- (dx*dy*md*mp)/(md + mp) + (JDXX - JDYY)*Cos(disk)*Sin(disk)) + (-JPXZ +
&
(dx*dz*md*mp)/(md + mp))*Sin(phi),2) + ((JPXX + ((Power(dy,2) +  &
Power(dz,2))*md*mp)/(md + mp) + JDXX*Power(Cos(disk),2) +  &
JDYY*Power(Sin(disk),2))*(Power(Cos(phi),2)*(JPYY*md + JPYY*mp +  &
Power(dx,2)*md*mp + Power(dz,2)*md*mp + JDYY*(md +
mp)*Power(Cos(disk),2) +  &
JDXX*(md + mp)*Power(Sin(disk),2)) + Sin(phi)*(2*dy*dz*md*mp*Cos(phi) +
&
((Power(dx,2) + Power(dy,2))*md*mp + JDYY*(md + mp) + JPYY*(md +  &
mp))*Sin(phi)) - JPYZ*(md + mp)*Sin(2*phi)))/(md + mp))) +  &
((-((Cos(phi)*(JPXY - (dx*dy*md*mp)/(md + mp) + (JDXX -  &
```

```
JDYY)*Cos(disk)*Sin(disk)) + (-JPXZ + (dx*dz*md*mp)/(md +  &
mp))*Sin(phi))*((JPXZ - (dx*dz*md*mp)/(md + mp))*Cos(phi) + (JPXY -  &
(dx*dy*md*mp)/(md + mp) + (JDXX - JDYY)*Cos(disk)*Sin(disk))*Sin(phi))) +
&
((JPXX + ((Power(dy,2) + Power(dz,2))*md*mp)/(md + mp) +  &
JDXX*Power(Cos(disk),2) + JDYY*Power(Sin(disk),2))*((-(dy*dz*md*mp) +  &
JPYZ*(md + mp))*Power(Cos(phi),2) + Cos(phi)*(-(JDYY*md) - JDYY*mp -  &
Power(dy,2)*md*mp + Power(dz,2)*md*mp + JDYY*(md +
mp)*Power(Cos(disk),2) +  &
JDXX*(md + mp)*Power(Sin(disk),2))*Sin(phi) - (-(dy*dz*md*mp) + JPYZ*(md
+  &
mp))*Power(Sin(phi),2)))/(md + mp))*(-((-(((Cos(phi)*(JPXY -
(dx*dy*md*mp)/(md  &
+ mp) + (JDXX - JDYY)*Cos(disk)*Sin(disk)) + (-JPXZ + (dx*dz*md*mp)/(md
+  &
mp))*Sin(phi))*((JPXZ - (dx*dz*md*mp)/(md + mp))*Cos(phi) + (JPXY -  &
(dx*dy*md*mp)/(md + mp) + (JDXX - JDYY)*Cos(disk)*Sin(disk))*Sin(phi))) +
&
((JPXX + ((Power(dy,2) + Power(dz,2))*md*mp)/(md + mp) +  &
JDXX*Power(Cos(disk),2) + JDYY*Power(Sin(disk),2))*((-(dy*dz*md*mp) +  &
JPYZ*(md + mp))*Power(Cos(phi),2) + Cos(phi)*(-(JDYY*md) - JDYY*mp -  &
Power(dy,2)*md*mp + Power(dz,2)*md*mp + JDYY*(md +
mp)*Power(Cos(disk),2) +  &
JDXX*(md + mp)*Power(Sin(disk),2))*Sin(phi) - (-(dy*dz*md*mp) + JPYZ*(md
+  &
mp))*Power(Sin(phi),2)))/(md + mp))*(-((Cos(phi)*(JPXY - (dx*dy*md*mp)/(md
+  &
mp) + (JDXX - JDYY)*Cos(disk)*Sin(disk)) + (-JPXZ + (dx*dz*md*mp)/(md +
&
mp))*Sin(phi))*(-(CYPA*D*dz*md*pt*rho*S*Cos(phi))/(4.*(md + mp)) -  &
(CNA*dy*md*rho*S*V*Cos(phi))/(2.*(md + mp)) -  &
(CYPA*D*dy*md*pt*rho*S*Sin(phi))/(4.*(md + mp)) +  &
(CNA*dz*md*rho*S*V*Sin(phi))/(2.*(md + mp)))) + (JPXX + ((Power(dy,2) +
&
Power(dz,2))*md*mp)/(md + mp) + JDXX*Power(Cos(disk),2) +  &
JDYY*Power(Sin(disk),2))*(-(CNA*dax*rho*S*V)/2. +  &
(CNA*dx*md*rho*S*V*Power(Cos(phi),2))/(2.*(md + mp)) +  &
(CNA*dx*md*rho*S*V*Power(Sin(phi),2))/(2.*(md + mp))))) +  &
(-((-(CYPA*D*dz*md*pt*rho*S*Cos(phi))/(4.*(md + mp)) -  &
(CNA*dy*md*rho*S*V*Cos(phi))/(2.*(md + mp)) -  &
(CYPA*D*dy*md*pt*rho*S*Sin(phi))/(4.*(md + mp)) +  &
(CNA*dz*md*rho*S*V*Sin(phi))/(2.*(md + mp)))*((JPXZ -
(dx*dz*md*mp)/(md +  &
mp))*Cos(phi) + (JPXY - (dx*dy*md*mp)/(md + mp) + (JDXX -  &
JDYY)*Cos(disk)*Sin(disk))*Sin(phi))) + (JPXX + ((Power(dy,2) +  &
Power(dz,2))*md*mp)/(md + mp) + JDXX*Power(Cos(disk),2) +  &
```

```
JDYY*Power(Sin(disk),2))*(-(CYPA*D*dmx*pt*rho*S)/4. +  &
(CYPA*D*dx*md*pt*rho*S*Power(Cos(phi),2))/(4.*(md + mp)) +  &
(CYPA*D*dx*md*pt*rho*S*Power(Sin(phi),2))/(4.*(md +  &
mp))))*(-Power(Cos(phi)*(JPXY - (dx*dy*md*mp)/(md + mp) + (JDXX -  &
JDYY)*Cos(disk)*Sin(disk)) + (-JPXZ + (dx*dz*md*mp)/(md + mp))*Sin(phi),2)
+  &
((JPXX + ((Power(dy,2) + Power(dz,2))*md*mp)/(md + mp) +  &
JDXX*Power(Cos(disk),2) +  &
JDYY*Power(Sin(disk),2))*(Power(Cos(phi),2)*(JPYY*md + JPYY*mp +  &
Power(dx,2)*md*mp + Power(dz,2)*md*mp + JDYY*(md +
mp)*Power(Cos(disk),2) +  &
JDXX*(md + mp)*Power(Sin(disk),2)) + Sin(phi)*(2*dy*dz*md*mp*Cos(phi) +
&
((Power(dx,2) + Power(dy,2))*md*mp + JDYY*(md + mp) + JPYY*(md +  &
mp))*Sin(phi)) - JPYZ*(md + mp)*Sin(2*phi)))/(md +  &
mp))))/((-Power(Cos(phi)*(JPXY - (dx*dy*md*mp)/(md + mp) + (JDXX -  &
JDYY)*Cos(disk)*Sin(disk)) + (-JPXZ + (dx*dz*md*mp)/(md + mp))*Sin(phi),2)
+  &
((JPXX + ((Power(dy,2) + Power(dz,2))*md*mp)/(md + mp) +  &
JDXX*Power(Cos(disk),2) +  &
JDYY*Power(Sin(disk),2))*(Power(Cos(phi),2)*(JPYY*md + JPYY*mp +  &
Power(dx,2)*md*mp + Power(dz,2)*md*mp + JDYY*(md +
mp)*Power(Cos(disk),2) +  &
JDXX*(md + mp)*Power(Sin(disk),2)) + Sin(phi)*(2*dy*dz*md*mp*Cos(phi) +
&
((Power(dx,2) + Power(dy,2))*md*mp + JDYY*(md + mp) + JPYY*(md +  &
mp))*Sin(phi)) - JPYZ*(md + mp)*Sin(2*phi)))/(md +  &
mp))*(-Power(-((Cos(phi)*(JPXY - (dx*dy*md*mp)/(md + mp) + (JDXX -  &
JDYY)*Cos(disk)*Sin(disk)) + (-JPXZ + (dx*dz*md*mp)/(md +  &
mp))*Sin(phi))*((JPXZ - (dx*dz*md*mp)/(md + mp))*Cos(phi) + (JPXY -  &
(dx*dy*md*mp)/(md + mp) + (JDXX - JDYY)*Cos(disk)*Sin(disk))*Sin(phi))) +
&
((JPXX + ((Power(dy,2) + Power(dz,2))*md*mp)/(md + mp) +  &
JDXX*Power(Cos(disk),2) + JDYY*Power(Sin(disk),2))*((-(dy*dz*md*mp) +  &
JPYZ*(md + mp))*Power(Cos(phi),2) + Cos(phi)*(-(JDYY*md) - JDYY*mp -  &
Power(dy,2)*md*mp + Power(dz,2)*md*mp + JDYY*(md +
mp)*Power(Cos(disk),2) +  &
JDXX*(md + mp)*Power(Sin(disk),2))*Sin(phi) - (-(dy*dz*md*mp) + JPYZ*(md
+  &
mp))*Power(Sin(phi),2)))/(md + mp),2) + (-Power(Cos(phi)*(JPXY -  &
(dx*dy*md*mp)/(md + mp) + (JDXX - JDYY)*Cos(disk)*Sin(disk)) + (-JPXZ +
&
(dx*dz*md*mp)/(md + mp))*Sin(phi),2) + ((JPXX + ((Power(dy,2) +  &
Power(dz,2))*md*mp)/(md + mp) + JDXX*Power(Cos(disk),2) +  &
JDYY*Power(Sin(disk),2))*(Power(Cos(phi),2)*(JPYY*md + JPYY*mp +  &
Power(dx,2)*md*mp + Power(dz,2)*md*mp + JDYY*(md +
```

```
mp)*Power(Cos(disk),2) +  &
JDXX*(md + mp)*Power(Sin(disk),2)) + Sin(phi)*(2*dy*dz*md*mp*Cos(phi) +
&
((Power(dx,2) + Power(dy,2))*md*mp + JDYY*(md + mp) + JPYY*(md +  &
mp))*Sin(phi)) - JPYZ*(md + mp)*Sin(2*phi)))/(md + mp))*(-Power((JPXZ -  &
(dx*dz*md*mp)/(md + mp))*Cos(phi) + (JPXY - (dx*dy*md*mp)/(md + mp) +
(JDXX -  &
JDYY)*Cos(disk)*Sin(disk))*Sin(phi),2) + ((JPXX + ((Power(dy,2) +  &
Power(dz,2))*md*mp)/(md + mp) + JDXX*Power(Cos(disk),2) +  &
JDYY*Power(Sin(disk),2))*(((Power(dx,2) + Power(dy,2))*md*mp + JDYY*(md
+ mp)  &
+ JPYY*(md + mp))*Power(Cos(phi),2) - 2*dy*dz*md*mp*Cos(phi)*Sin(phi) +
&
(JPYY*md + JPYY*mp + Power(dx,2)*md*mp + Power(dz,2)*md*mp +
JDYY*(md +  &
mp)*Power(Cos(disk),2) + JDXX*(md +
mp)*Power(Sin(disk),2))*Power(Sin(phi),2)  &
+ JPYZ*(md + mp)*Sin(2*phi)))/(md + mp))))))/V
```

A4) $D = D$

A5)
```
E =  (D*(-((-(((Cos(phi)*(JPXY - (dx*dy*md*mp)/(md + mp) + (JDXX -  &
JDYY)*Cos(disk)*Sin(disk)) + (-JPXZ + (dx*dz*md*mp)/(md +  &
mp))*Sin(phi))*(JDXX*omega*Power(Cos(disk),2)*Sin(disk)*Sin(phi) +  &
JDXX*omega*Power(Sin(disk),3)*Sin(phi))) + (JPXX + ((Power(dy,2) +  &
Power(dz,2))*md*mp)/(md + mp) + JDXX*Power(Cos(disk),2) +  &
JDYY*Power(Sin(disk),2))*(-(CMQ*Power(D,2)*rho*S*V)/4. -  &
2*JPYZ*pt*Power(Cos(phi),2) + (2*dy*dz*md*mp*pt*Power(Cos(phi),2))/(md +
mp)  &
+ 2*JDYY*pt*Cos(phi)*Sin(phi) +  &
(2*Power(dy,2)*md*mp*pt*Cos(phi)*Sin(phi))/(md + mp) -  &
(2*Power(dz,2)*md*mp*pt*Cos(phi)*Sin(phi))/(md + mp) -  &
2*JDYY*pt*Power(Cos(disk),2)*Cos(phi)*Sin(phi) -  &
2*JDXX*pt*Cos(phi)*Power(Sin(disk),2)*Sin(phi) +
2*JPYZ*pt*Power(Sin(phi),2)  &
- (2*dy*dz*md*mp*pt*Power(Sin(phi),2))/(md + mp)))/(-Power(Cos(phi)*(JPXY
-  &
(dx*dy*md*mp)/(md + mp) + (JDXX - JDYY)*Cos(disk)*Sin(disk)) + (-JPXZ +
&
(dx*dz*md*mp)/(md + mp))*Sin(phi),2) + ((JPXX + ((Power(dy,2) +  &
Power(dz,2))*md*mp)/(md + mp) + JDXX*Power(Cos(disk),2) +  &
JDYY*Power(Sin(disk),2))*(Power(Cos(phi),2)*(JPYY*md + JPYY*mp +  &
Power(dx,2)*md*mp + Power(dz,2)*md*mp + JDYY*(md +
mp)*Power(Cos(disk),2) +  &
```

```
JDXX*(md + mp)*Power(Sin(disk),2)) + Sin(phi)*(2*dy*dz*md*mp*Cos(phi) +
&
((Power(dx,2) + Power(dy,2))*md*mp + JDYY*(md + mp) + JPYY*(md +  &
mp))*Sin(phi)) - JPYZ*(md + mp)*Sin(2*phi)))/(md + mp))) +  &
((-((Cos(phi)*(JPXY - (dx*dy*md*mp)/(md + mp) + (JDXX -  &
JDYY)*Cos(disk)*Sin(disk)) + (-JPXZ + (dx*dz*md*mp)/(md +  &
mp))*Sin(phi))*((JPXZ - (dx*dz*md*mp)/(md + mp))*Cos(phi) + (JPXY -  &
(dx*dy*md*mp)/(md + mp) + (JDXX - JDYY)*Cos(disk)*Sin(disk))*Sin(phi))) +
&
((JPXX + ((Power(dy,2) + Power(dz,2))*md*mp)/(md + mp) +  &
JDXX*Power(Cos(disk),2) + JDYY*Power(Sin(disk),2))*((-(dy*dz*md*mp) +  &
JPYZ*(md + mp))*Power(Cos(phi),2) + Cos(phi)*(-(JDYY*md) - JDYY*mp -  &
Power(dy,2)*md*mp + Power(dz,2)*md*mp + JDYY*(md +
mp)*Power(Cos(disk),2) +  &
JDXX*(md + mp)*Power(Sin(disk),2))*Sin(phi) - (-(dy*dz*md*mp) + JPYZ*(md
+  &
mp))*Power(Sin(phi),2)))/(md + mp))*(-((-((Cos(phi)*(JPXY -
(dx*dy*md*mp)/(md  &
+ mp) + (JDXX - JDYY)*Cos(disk)*Sin(disk)) + (-JPXZ + (dx*dz*md*mp)/(md
+  &
mp))*Sin(phi))*((JPXZ - (dx*dz*md*mp)/(md + mp))*Cos(phi) + (JPXY -  &
(dx*dy*md*mp)/(md + mp) + (JDXX - JDYY)*Cos(disk)*Sin(disk))*Sin(phi))) +
&
((JPXX + ((Power(dy,2) + Power(dz,2))*md*mp)/(md + mp) +  &
JDXX*Power(Cos(disk),2) + JDYY*Power(Sin(disk),2))*((-(dy*dz*md*mp) +  &
JPYZ*(md + mp))*Power(Cos(phi),2) + Cos(phi)*(-(JDYY*md) - JDYY*mp -  &
Power(dy,2)*md*mp + Power(dz,2)*md*mp + JDYY*(md +
mp)*Power(Cos(disk),2) +  &
JDXX*(md + mp)*Power(Sin(disk),2))*Sin(phi) - (-(dy*dz*md*mp) + JPYZ*(md
+  &
mp))*Power(Sin(phi),2)))/(md + mp))*(-((Cos(phi)*(JPXY - (dx*dy*md*mp)/(md
+  &
mp) + (JDXX - JDYY)*Cos(disk)*Sin(disk)) + (-JPXZ + (dx*dz*md*mp)/(md +
&
mp))*Sin(phi))*(JDXX*omega*Power(Cos(disk),2)*Sin(disk)*Sin(phi) +  &
JDXX*omega*Power(Sin(disk),3)*Sin(phi))) + (JPXX + ((Power(dy,2) +  &
Power(dz,2))*md*mp)/(md + mp) + JDXX*Power(Cos(disk),2) +  &
JDYY*Power(Sin(disk),2))*(-(CMQ*Power(D,2)*rho*S*V)/4. -  &
2*JPYZ*pt*Power(Cos(phi),2) + (2*dy*dz*md*mp*pt*Power(Cos(phi),2))/(md +
mp)  &
+ 2*JDYY*pt*Cos(phi)*Sin(phi) +  &
(2*Power(dy,2)*md*mp*pt*Cos(phi)*Sin(phi))/(md + mp) -  &
(2*Power(dz,2)*md*mp*pt*Cos(phi)*Sin(phi))/(md + mp) -  &
2*JDYY*pt*Power(Cos(disk),2)*Cos(phi)*Sin(phi) -  &
2*JDXX*pt*Cos(phi)*Power(Sin(disk),2)*Sin(phi) +
2*JPYZ*pt*Power(Sin(phi),2)  &
```

```
- (2*dy*dz*md*mp*pt*Power(Sin(phi),2))/(md + mp)))) +  &
(-((JDXX*omega*Power(Cos(disk),2)*Sin(disk)*Sin(phi) +  &
JDXX*omega*Power(Sin(disk),3)*Sin(phi))*((JPXZ - (dx*dz*md*mp)/(md +  &
mp))*Cos(phi) + (JPXY - (dx*dy*md*mp)/(md + mp) + (JDXX -  &
JDYY)*Cos(disk)*Sin(disk))*Sin(phi))) + (JPXX + ((Power(dy,2) +  &
Power(dz,2))*md*mp)/(md + mp) + JDXX*Power(Cos(disk),2) +  &
JDYY*Power(Sin(disk),2))*(-(JDYY*pt*Power(Cos(phi),2)) -  &
JPXX*pt*Power(Cos(phi),2) -
(2*Power(dy,2)*md*mp*pt*Power(Cos(phi),2))/(md +  &
mp) - JDXX*pt*Power(Cos(disk),2)*Power(Cos(phi),2) +  &
JDYY*pt*Power(Cos(disk),2)*Power(Cos(phi),2) -  &
JDXX*omega*Power(Cos(disk),3)*Power(Cos(phi),2) +  &
JDXX*pt*Power(Cos(phi),2)*Power(Sin(disk),2) -  &
JDYY*pt*Power(Cos(phi),2)*Power(Sin(disk),2) -  &
JDXX*omega*Cos(disk)*Power(Cos(phi),2)*Power(Sin(disk),2) -  &
4*JPYZ*pt*Cos(phi)*Sin(phi) + (4*dy*dz*md*mp*pt*Cos(phi)*Sin(phi))/(md +
mp)  &
+ JDYY*pt*Power(Sin(phi),2) - JPXX*pt*Power(Sin(phi),2) -  &
(2*Power(dz,2)*md*mp*pt*Power(Sin(phi),2))/(md + mp) -  &
JDXX*pt*Power(Cos(disk),2)*Power(Sin(phi),2) -  &
JDYY*pt*Power(Cos(disk),2)*Power(Sin(phi),2) -  &
JDXX*omega*Power(Cos(disk),3)*Power(Sin(phi),2) -  &
JDXX*pt*Power(Sin(disk),2)*Power(Sin(phi),2) -  &
JDYY*pt*Power(Sin(disk),2)*Power(Sin(phi),2) -  &
JDXX*omega*Cos(disk)*Power(Sin(disk),2)*Power(Sin(phi),2)))*(-
Power(Cos(phi)*( &
JPXY - (dx*dy*md*mp)/(md + mp) + (JDXX - JDYY)*Cos(disk)*Sin(disk)) + (-
JPXZ  &
+ (dx*dz*md*mp)/(md + mp))*Sin(phi),2) + ((JPXX + ((Power(dy,2) +  &
Power(dz,2))*md*mp)/(md + mp) + JDXX*Power(Cos(disk),2) +  &
JDYY*Power(Sin(disk),2))*(Power(Cos(phi),2)*(JPYY*md + JPYY*mp +  &
Power(dx,2)*md*mp + Power(dz,2)*md*mp + JDYY*(md +
mp)*Power(Cos(disk),2) +  &
JDXX*(md + mp)*Power(Sin(disk),2)) + Sin(phi)*(2*dy*dz*md*mp*Cos(phi) +
&
((Power(dx,2) + Power(dy,2))*md*mp + JDYY*(md + mp) + JPYY*(md +  &
mp))*Sin(phi)) - JPYZ*(md + mp)*Sin(2*phi)))/(md +  &
mp))))/((-Power(Cos(phi)*(JPXY - (dx*dy*md*mp)/(md + mp) + (JDXX -  &
JDYY)*Cos(disk)*Sin(disk)) + (-JPXZ + (dx*dz*md*mp)/(md + mp))*Sin(phi),2)
+  &
((JPXX + ((Power(dy,2) + Power(dz,2))*md*mp)/(md + mp) +  &
JDXX*Power(Cos(disk),2) +  &
JDYY*Power(Sin(disk),2))*(Power(Cos(phi),2)*(JPYY*md + JPYY*mp +  &
Power(dx,2)*md*mp + Power(dz,2)*md*mp + JDYY*(md +
mp)*Power(Cos(disk),2) +  &
JDXX*(md + mp)*Power(Sin(disk),2)) + Sin(phi)*(2*dy*dz*md*mp*Cos(phi) +
```

```
&
((Power(dx,2) + Power(dy,2))*md*mp + JDYY*(md + mp) + JPYY*(md +  &
mp))*Sin(phi)) - JPYZ*(md + mp)*Sin(2*phi)))/(md +  &
mp))*(-Power(-((Cos(phi)*(JPXY - (dx*dy*md*mp)/(md + mp) + (JDXX -  &
JDYY)*Cos(disk)*Sin(disk)) + (-JPXZ + (dx*dz*md*mp)/(md +  &
mp))*Sin(phi))*((JPXZ - (dx*dz*md*mp)/(md + mp))*Cos(phi) + (JPXY -  &
(dx*dy*md*mp)/(md + mp) + (JDXX - JDYY)*Cos(disk)*Sin(disk))*Sin(phi))) +
&
((JPXX + ((Power(dy,2) + Power(dz,2))*md*mp)/(md + mp) +  &
JDXX*Power(Cos(disk),2) + JDYY*Power(Sin(disk),2))*((-(dy*dz*md*mp) +  &
JPYZ*(md + mp))*Power(Cos(phi),2) + Cos(phi)*(-(JDYY*md) - JDYY*mp -  &
Power(dy,2)*md*mp + Power(dz,2)*md*mp + JDYY*(md +
mp)*Power(Cos(disk),2) +  &
JDXX*(md + mp)*Power(Sin(disk),2))*Sin(phi) - (-(dy*dz*md*mp) + JPYZ*(md
+  &
mp))*Power(Sin(phi),2)))/(md + mp),2) + (-Power(Cos(phi)*(JPXY -  &
(dx*dy*md*mp)/(md + mp) + (JDXX - JDYY)*Cos(disk)*Sin(disk)) + (-JPXZ +
&
(dx*dz*md*mp)/(md + mp))*Sin(phi),2) + ((JPXX + ((Power(dy,2) +  &
Power(dz,2))*md*mp)/(md + mp) + JDXX*Power(Cos(disk),2) +  &
JDYY*Power(Sin(disk),2))*(Power(Cos(phi),2)*(JPYY*md + JPYY*mp +  &
Power(dx,2)*md*mp + Power(dz,2)*md*mp + JDYY*(md +
mp)*Power(Cos(disk),2) +  &
JDXX*(md + mp)*Power(Sin(disk),2)) + Sin(phi)*(2*dy*dz*md*mp*Cos(phi) +
&
((Power(dx,2) + Power(dy,2))*md*mp + JDYY*(md + mp) + JPYY*(md +  &
mp))*Sin(phi)) - JPYZ*(md + mp)*Sin(2*phi)))/(md + mp))*(-Power((JPXZ -  &
(dx*dz*md*mp)/(md + mp))*Cos(phi) + (JPXY - (dx*dy*md*mp)/(md + mp) +
(JDXX -  &
JDYY)*Cos(disk)*Sin(disk))*Sin(phi),2) + ((JPXX + ((Power(dy,2) +  &
Power(dz,2))*md*mp)/(md + mp) + JDXX*Power(Cos(disk),2) +  &
JDYY*Power(Sin(disk),2))*(((Power(dx,2) + Power(dy,2))*md*mp + JDYY*(md
+ mp)  &
+ JPYY*(md + mp))*Power(Cos(phi),2) - 2*dy*dz*md*mp*Cos(phi)*Sin(phi) +
&
(JPYY*md + JPYY*mp + Power(dx,2)*md*mp + Power(dz,2)*md*mp +
JDYY*(md +  &
mp)*Power(Cos(disk),2) + JDXX*(md +
mp)*Power(Sin(disk),2))*Power(Sin(phi),2)  &
+ JPYZ*(md + mp)*Sin(2*phi)))/(md + mp))))))/V
```

A6) $F =$

```
-((D*(-((-((Cos(phi)*(JPXY - (dx*dy*md*mp)/(md + mp) + (JDXX -  &
JDYY)*Cos(disk)*Sin(disk)) + (-JPXZ + (dx*dz*md*mp)/(md +  &
mp))*Sin(phi))*((JPXZ - (dx*dz*md*mp)/(md + mp))*Cos(phi) + (JPXY -  &
(dx*dy*md*mp)/(md + mp) + (JDXX - JDYY)*Cos(disk)*Sin(disk))*Sin(phi))) +
```

```
&
((JPXX + ((Power(dy,2) + Power(dz,2))*md*mp)/(md + mp) +  &
JDXX*Power(Cos(disk),2) + JDYY*Power(Sin(disk),2))*((-(dy*dz*md*mp) +  &
JPYZ*(md + mp))*Power(Cos(phi),2) + Cos(phi)*(-(JDYY*md) - JDYY*mp -  &
Power(dy,2)*md*mp + Power(dz,2)*md*mp + JDYY*(md +
mp)*Power(Cos(disk),2) +  &
JDXX*(md + mp)*Power(Sin(disk),2))*Sin(phi) - (-(dy*dz*md*mp) + JPYZ*(md
+  &
mp))*Power(Sin(phi),2)))/(md + mp))*(-((Cos(phi)*(JPXY - (dx*dy*md*mp)/(md
+  &
mp) + (JDXX - JDYY)*Cos(disk)*Sin(disk)) + (-JPXZ + (dx*dz*md*mp)/(md +
&
mp))*Sin(phi))*(JDXX*omega*Power(Cos(disk),2)*Sin(disk)*Sin(phi) +  &
JDXX*omega*Power(Sin(disk),3)*Sin(phi))) + (JPXX + ((Power(dy,2) +  &
Power(dz,2))*md*mp)/(md + mp) + JDXX*Power(Cos(disk),2) +  &
JDYY*Power(Sin(disk),2))*(-(CMQ*Power(D,2)*rho*S*V)/4. -  &
2*JPYZ*pt*Power(Cos(phi),2) + (2*dy*dz*md*mp*pt*Power(Cos(phi),2))/(md +
mp)  &
+ 2*JDYY*pt*Cos(phi)*Sin(phi) +  &
(2*Power(dy,2)*md*mp*pt*Cos(phi)*Sin(phi))/(md + mp) -  &
(2*Power(dz,2)*md*mp*pt*Cos(phi)*Sin(phi))/(md + mp) -  &
2*JDYY*pt*Power(Cos(disk),2)*Cos(phi)*Sin(phi) -  &
2*JDXX*pt*Cos(phi)*Power(Sin(disk),2)*Sin(phi) +
2*JPYZ*pt*Power(Sin(phi),2)  &
- (2*dy*dz*md*mp*pt*Power(Sin(phi),2))/(md + mp)))) +  &
(-((JDXX*omega*Power(Cos(disk),2)*Sin(disk)*Sin(phi) +  &
JDXX*omega*Power(Sin(disk),3)*Sin(phi))*((JPXZ - (dx*dz*md*mp)/(md +  &
mp))*Cos(phi) + (JPXY - (dx*dy*md*mp)/(md + mp) + (JDXX -  &
JDYY)*Cos(disk)*Sin(disk))*Sin(phi))) + (JPXX + ((Power(dy,2) +  &
Power(dz,2))*md*mp)/(md + mp) + JDXX*Power(Cos(disk),2) +  &
JDYY*Power(Sin(disk),2))*(-(JDYY*pt*Power(Cos(phi),2)) -  &
JPXX*pt*Power(Cos(phi),2) -
(2*Power(dy,2)*md*mp*pt*Power(Cos(phi),2))/(md +  &
mp) - JDXX*pt*Power(Cos(disk),2)*Power(Cos(phi),2) +  &
JDYY*pt*Power(Cos(disk),2)*Power(Cos(phi),2) -  &
JDXX*omega*Power(Cos(disk),3)*Power(Cos(phi),2) +  &
JDXX*pt*Power(Cos(phi),2)*Power(Sin(disk),2) -  &
JDYY*pt*Power(Cos(phi),2)*Power(Sin(disk),2) -  &
JDXX*omega*Cos(disk)*Power(Cos(phi),2)*Power(Sin(disk),2) -  &
4*JPYZ*pt*Cos(phi)*Sin(phi) + (4*dy*dz*md*mp*pt*Cos(phi)*Sin(phi))/(md +
mp)  &
+ JDYY*pt*Power(Sin(phi),2) - JPXX*pt*Power(Sin(phi),2) -  &
(2*Power(dz,2)*md*mp*pt*Power(Sin(phi),2))/(md + mp) -  &
JDXX*pt*Power(Cos(disk),2)*Power(Sin(phi),2) -  &
JDYY*pt*Power(Cos(disk),2)*Power(Sin(phi),2) -  &
JDXX*omega*Power(Cos(disk),3)*Power(Sin(phi),2) -  &
```

```
JDXX*pt*Power(Sin(disk),2)*Power(Sin(phi),2) -  &
JDYY*pt*Power(Sin(disk),2)*Power(Sin(phi),2) -  &
JDXX*omega*Cos(disk)*Power(Sin(disk),2)*Power(Sin(phi),2)))*(-
Power(Cos(phi)*( &
JPXY - (dx*dy*md*mp)/(md + mp) + (JDXX - JDYY)*Cos(disk)*Sin(disk)) + (-
JPXZ  &
+ (dx*dz*md*mp)/(md + mp))*Sin(phi),2) + ((JPXX + ((Power(dy,2) +  &
Power(dz,2))*md*mp)/(md + mp) + JDXX*Power(Cos(disk),2) +  &
JDYY*Power(Sin(disk),2))*(Power(Cos(phi),2)*(JPYY*md + JPYY*mp +  &
Power(dx,2)*md*mp + Power(dz,2)*md*mp + JDYY*(md +
mp)*Power(Cos(disk),2) +  &
JDXX*(md + mp)*Power(Sin(disk),2)) + Sin(phi)*(2*dy*dz*md*mp*Cos(phi) +
&
((Power(dx,2) + Power(dy,2))*md*mp + JDYY*(md + mp) + JPYY*(md +  &
mp))*Sin(phi)) - JPYZ*(md + mp)*Sin(2*phi)))/(md +  &
mp))))/(V*(-Power(-((Cos(phi)*(JPXY - (dx*dy*md*mp)/(md + mp) + (JDXX -
&
JDYY)*Cos(disk)*Sin(disk)) + (-JPXZ + (dx*dz*md*mp)/(md +  &
mp))*Sin(phi))*((JPXZ - (dx*dz*md*mp)/(md + mp))*Cos(phi) + (JPXY -  &
(dx*dy*md*mp)/(md + mp) + (JDXX - JDYY)*Cos(disk)*Sin(disk))*Sin(phi))) +
&
((JPXX + ((Power(dy,2) + Power(dz,2))*md*mp)/(md + mp) +  &
JDXX*Power(Cos(disk),2) + JDYY*Power(Sin(disk),2))*((-(dy*dz*md*mp) +  &
JPYZ*(md + mp))*Power(Cos(phi),2) + Cos(phi)*(-(JDYY*md) - JDYY*mp -  &
Power(dy,2)*md*mp + Power(dz,2)*md*mp + JDYY*(md +
mp)*Power(Cos(disk),2) +  &
JDXX*(md + mp)*Power(Sin(disk),2))*Sin(phi) - (-(dy*dz*md*mp) + JPYZ*(md
+  &
mp))*Power(Sin(phi),2)))/(md + mp),2) + (-Power(Cos(phi)*(JPXY -  &
(dx*dy*md*mp)/(md + mp) + (JDXX - JDYY)*Cos(disk)*Sin(disk)) + (-JPXZ +
&
(dx*dz*md*mp)/(md + mp))*Sin(phi),2) + ((JPXX + ((Power(dy,2) +  &
Power(dz,2))*md*mp)/(md + mp) + JDXX*Power(Cos(disk),2) +  &
JDYY*Power(Sin(disk),2))*(Power(Cos(phi),2)*(JPYY*md + JPYY*mp +  &
Power(dx,2)*md*mp + Power(dz,2)*md*mp + JDYY*(md +
mp)*Power(Cos(disk),2) +  &
JDXX*(md + mp)*Power(Sin(disk),2)) + Sin(phi)*(2*dy*dz*md*mp*Cos(phi) +
&
((Power(dx,2) + Power(dy,2))*md*mp + JDYY*(md + mp) + JPYY*(md +  &
mp))*Sin(phi)) - JPYZ*(md + mp)*Sin(2*phi)))/(md + mp))*(-Power((JPXZ -  &
(dx*dz*md*mp)/(md + mp))*Cos(phi) + (JPXY - (dx*dy*md*mp)/(md + mp) +
(JDXX -  &
JDYY)*Cos(disk)*Sin(disk))*Sin(phi),2) + ((JPXX + ((Power(dy,2) +  &
Power(dz,2))*md*mp)/(md + mp) + JDXX*Power(Cos(disk),2) +  &
JDYY*Power(Sin(disk),2))*(((Power(dx,2) + Power(dy,2))*md*mp + JDYY*(md
+ mp)  &
```

```
+ JPYY*(md + mp))*Power(Cos(phi),2) - 2*dy*dz*md*mp*Cos(phi)*Sin(phi) +
&
(JPYY*md + JPYY*mp + Power(dx,2)*md*mp + Power(dz,2)*md*mp +
JDYY*(md +  &
mp)*Power(Cos(disk),2) + JDXX*(md +
mp)*Power(Sin(disk),2))*Power(Sin(phi),2)  &
+ JPYZ*(md + mp)*Sin(2*phi)))/(md + mp)))))
```

Appendix B. Coefficients of the Epicyclic Dynamic Equations in Symbolic-Form for a Special Case

Application of the linear theory assumptions to the simplified system of a projectile containing a rotating internal part located on the projectile axis of symmetry at a disk angle, Ω, equal to 0º yields the coefficients of the epicyclic equations shown in equations B-1 through B-6:

$$A = -\frac{\rho SDC_{NA}}{2m_C}; \tag{B-1}$$

$$B = \left(\frac{\rho SD}{2m_C}\right)\left(\frac{m_C D}{I_{CYY}}\right)\left(\frac{\left(x_{PM} - x_{PD}\,\frac{m_D}{m_C}\right)C_{YPA}\,\tilde{p}}{2V}\right); \tag{B-2}$$

$$C = \left(\frac{\rho SD}{2m_C}\right)\left(\frac{m_C D}{I_{CYY}}\right)\left(\frac{\left(x_{PA} - x_{PD}\,\frac{m_D}{m_C}\right)C_{NA}}{2D}\right); \tag{B-3}$$

$$D = D; \tag{B-4}$$

$$E = \left(\frac{\rho SD}{2m_C}\right)\left(\frac{m_C D^2}{I_{CYY}}\right)\frac{C_{MQ}}{2}; \tag{B-5}$$

$$F = \left(\frac{D}{V}\right)\frac{I_{PXX}\,\tilde{p} + I_{DXX}\left(\tilde{p} + \Omega\right)}{I_{CYY}}. \tag{B-6}$$

Magnus force is assumed to be small in comparison to other aerodynamic forces and is dropped from equations B-1 through B-6. However, due to the magnitude amplification resulting from the cross product between Magnus force and its respective moment arm, the Magnus moment is retained in equation B-2. The equations for the simplified system previously presented are essentially the same as those derived for a dual-spin projectile by Costello and Peterson.[1] They are identical if the aerodynamic coefficients applied on the aft section of a dual-spin projectile are neglected.

[1] Costello, M.; Peterson, A. Linear Theory of a Dual Spin Projectile in Atmospheric Flight. *Journal of Guidance, Control, and Dynamics* **2000**, *23* (4), 789–797.

INTENTIONALLY LEFT BLANK.

List of Abbreviations and Symbols

$\vec{I}_I, \vec{J}_I, \vec{K}_I$	=	inertial frame unit vectors
$\vec{I}_B, \vec{J}_B, \vec{K}_B$	=	body frame unit vectors
$\vec{I}_N, \vec{J}_N, \vec{K}_N$	=	no-roll frame unit vectors
x_{PD}, y_{PD}, z_{PD}	=	body frame components of distance vector from projectile center of mass to disk center of mass
x_P, y_P, z_P	=	body frame components of distance vector from projectile base to projectile center of mass
x_D, y_D, z_D	=	body frame components of distance vector from projectile base to disk center of mass
x_E, y_E, z_E	=	nominal body frame components of distance vector from projectile base to projectile center of mass
x_{PA}, y_{PA}, z_{PA}	=	no-roll frame components of distance vector from projectile center of mass to center of pressure
x_{PM}, y_{PM}, z_{PM}	=	no-roll frame components of distance vector from projectile center of mass to Magnus center of pressure
u, v, w	=	translational velocity components of the two-body system center of mass resolved in the body frame
$\widetilde{u}, \widetilde{v}, \widetilde{w}$	=	translational velocity components of the two-body system center of mass resolved in the no-roll frame
p, q, r	=	roll, pitch, and yaw components of the angular velocity vector of projectile body expressed in the body frame
$\widetilde{p}, \widetilde{q}, \widetilde{r}$	=	roll, pitch, and yaw components of the angular velocity vector of projectile body expressed in the no-roll frame
ϕ, θ, ψ	=	Euler roll, pitch, and yaw angles
x, y, z	=	position vector components of the two-body system center of mass expressed in the inertial frame
$\vec{\omega}_{N/I}$	=	angular velocity vector of no-roll reference frame with respect to the inertial frame

$\vec{\omega}_{D/I}$	=	angular velocity vector of disk body with respect to the inertial frame
$\vec{\omega}_{D/P}$	=	angular velocity vector of disk body with respect to the projectile body frame
$\vec{\omega}_{B/I}$	=	angular velocity vector of projectile body with respect to the inertial frame
$\vec{v}_{C/I}$	=	translational velocity vector of two-body system with respect to the inertial frame
$\vec{a}_{C/I}$	=	translational acceleration vector of two-body system with respect to the inertial frame
m_D	=	disk body mass
m_P	=	projectile body mass
m_C	=	two-body system mass
m_E	=	nominal projectile mass
$\vec{a}_{D/I}$	=	translational acceleration vector of disk mass center with respect to the inertial frame
$\vec{a}_{P/I}$	=	translational acceleration vector of projectile body mass center with respect to the inertial frame
$\vec{W}_C$	=	weight vector of two-body system
$\vec{W}_P$	=	weight vector of projectile body
$\vec{W}_D$	=	weight vector of disk body
$\vec{F}_R$	=	reaction force vector
$\vec{\alpha}_{P/I}$	=	angular acceleration vector of projectile body with respect to the inertial frame
$\vec{r}_{P\to D}$	=	distance vector from projectile center of mass to disk center of mass
$\vec{F}_A$	=	aerodynamic forces vector
X_A, Y_A, Z_A	=	aerodynamic force vector components expressed in the body frame
$\widetilde{X}_A, \widetilde{Y}_A, \widetilde{Z}_A$	=	aerodynamic force vector components expressed in the no-roll frame
X_W, Y_W, Z_W	=	projectile weight vector components expressed in the body frame

$\widetilde{X}_W, \widetilde{Y}_W, \widetilde{Z}_W$ = projectile weight vector components expressed in the no-roll frame

$\widetilde{X}, \widetilde{Y}, \widetilde{Z}$ = total external force components on the projectile body expressed in the no-roll frame

T_N = transformation matrix from the body frame to the no-roll frame

L_R, M_R, N_R = reaction moment components due to cross product of distance vector from projectile center of mass to disk center of mass with reaction force vector expressed in the body frame

$\widetilde{L}_R, \widetilde{M}_R, \widetilde{N}_R$ = reaction moment components due to cross product of distance vector from projectile center of mass to disk center of mass with reaction force vector expressed in the fixed frame

$\vec{H}_{P/I}$ = angular momentum vector of the projectile body with respect to the inertial frame

$\vec{H}_{D/I}$ = angular momentum vector of the disk body with respect to the inertial frame

$\vec{M}_R$ = reaction moment vector

$\vec{M}_A$ = total aerodynamic moment vector

H_{Px}, H_{Py}, H_{Pz} = angular momentum derivative vector components of the projectile body expressed in the body frame

$\widetilde{H}_{Px}, \widetilde{H}_{Py}, \widetilde{H}_{Pz}$ = angular momentum derivative vector components of the projectile body expressed in the no-roll frame

H_{Dx}, H_{Dy}, H_{Dz} = angular momentum derivative vector components of the projectile body expressed in the body frame

$\widetilde{H}_{Dx}, \widetilde{H}_{Dy}, \widetilde{H}_{Dz}$ = angular momentum derivative vector components of the projectile body expressed in the no-roll frame

L_A, M_A, N_A = total aerodynamic moment vector components expressed in the body frame

$\widetilde{L}_A, \widetilde{M}_A, \widetilde{N}_A$ = total aerodynamic moment vector components expressed in the no-roll frame

I_P = mass moment of inertia of the projectile body about its mass center with respect to the body frame

I_D	=	mass moment of inertia of the disk body about its mass center with respect to the disk frame
I_E	=	nominal mass moment of inertia of the projectile body about its mass center with respect to the body frame
$\widetilde{L}, \widetilde{M}, \widetilde{N}$	=	total aerodynamic moment vector components expressed in the no-roll frame
C_{X0}	=	zero yaw axial force aerodynamic coefficient for the projectile body
C_{X0}	=	zero yaw axial force aerodynamic coefficient for the projectile body
C_{X2}	=	yaw drag axial force aerodynamic coefficient for the projectile body
C_{Y0}	=	trim side force aerodynamic coefficient for the projectile body
C_{YB1}	=	normal force aerodynamic coefficient along $\vec{J}_N$ axis for the projectile body
C_{Z0}	=	trim vertical force aerodynamic coefficient for the projectile body
C_{ZB1}	=	normal force aerodynamic coefficient along $\vec{K}_N$ axis for the projectile body
C_{YPA}	=	Magnus force aerodynamic coefficient for the projectile body
C_{DD}	=	roll moment aerodynamic coefficient due to fin cant for the projectile body
C_{LP}	=	roll damping moment aerodynamic coefficient due to fin cant for the projectile body
C_{MQ}	=	pitch damping moment aerodynamic coefficient due to fin cant for the projectile body
V	=	velocity magnitude
α	=	longitudinal aerodynamic angle of attack
β	=	lateral aerodynamic angle of attack
ρ	=	density of air

NO. OF COPIES	ORGANIZATION
2	DEFENSE TECHNICAL INFORMATION CENTER DTIC OCA 8725 JOHN J KINGMAN RD STE 0944 FT BELVOIR VA 22060-6218
1	COMMANDING GENERAL US ARMY MATERIEL CMD AMCRDA TF 5001 EISENHOWER AVE ALEXANDRIA VA 22333-0001
1	INST FOR ADVNCD TCHNLGY THE UNIV OF TEXAS AT AUSTIN 3925 W BRAKER LN STE 400 AUSTIN TX 78759-5316
1	US MILITARY ACADEMY MATH SCI CTR EXCELLENCE MADN MATH THAYER HALL WEST POINT NY 10996-1786
1	DIRECTOR US ARMY RESEARCH LAB AMSRL D DR D SMITH 2800 POWDER MILL RD ADELPHI MD 20783-1197
1	DIRECTOR US ARMY RESEARCH LAB AMSRL CS IS R 2800 POWDER MILL RD ADELPHI MD 20783-1197
3	DIRECTOR US ARMY RESEARCH LAB AMSRL CI OK TL 2800 POWDER MILL RD ADELPHI MD 20783-1197
3	DIRECTOR US ARMY RESEARCH LAB AMSRL CS IS T 2800 POWDER MILL RD ADELPHI MD 20783-1197

NO. OF COPIES	ORGANIZATION
	ABERDEEN PROVING GROUND
2	DIR USARL AMSRL CI LP (BLDG 305) AMSRL CI OK TP (BLDG 4600)